

Transport in Mesoscopic Devices and Quantum Dots

A.M. CHANG

Dept. of Physics, Duke University

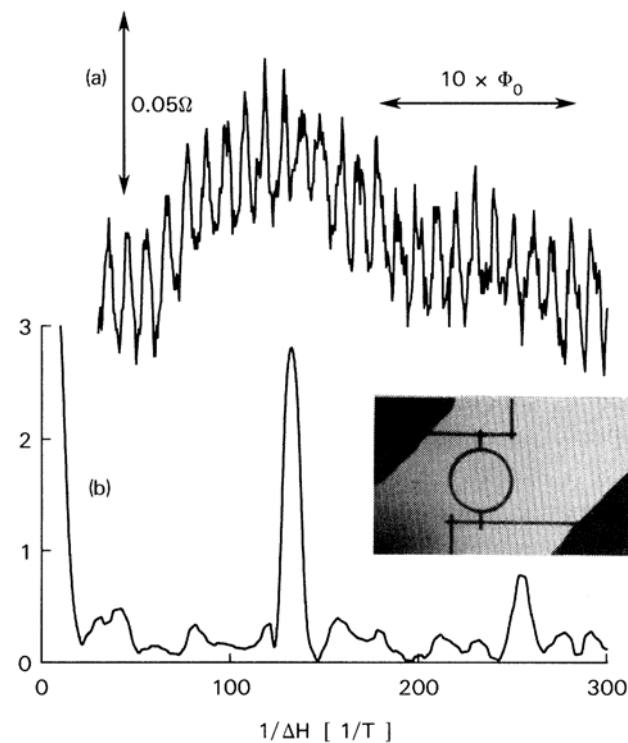
Academia Sinica, Taipei

National Tsing-Hua University, Hsinchu

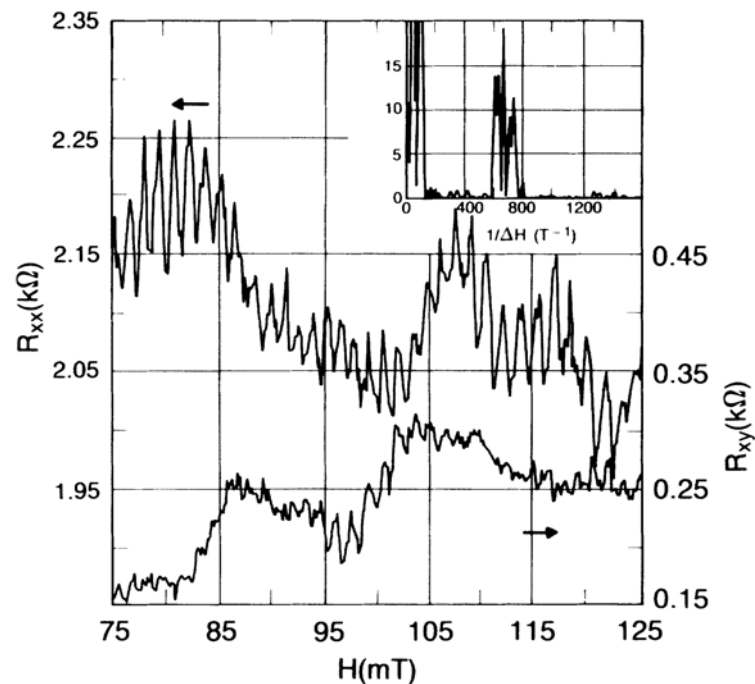
Mesoscopic

- Between microscopic (quantum mechanics of few atoms) and Macrosopic
- Quantum Interference
- Quantum Coherence

Metallic Rings— R.A. Webb, PRL 1985

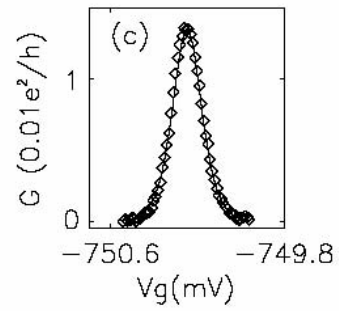
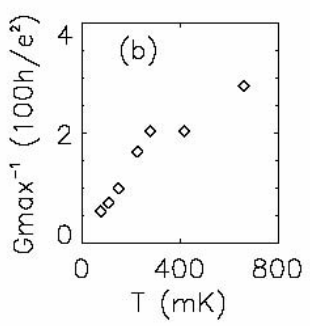
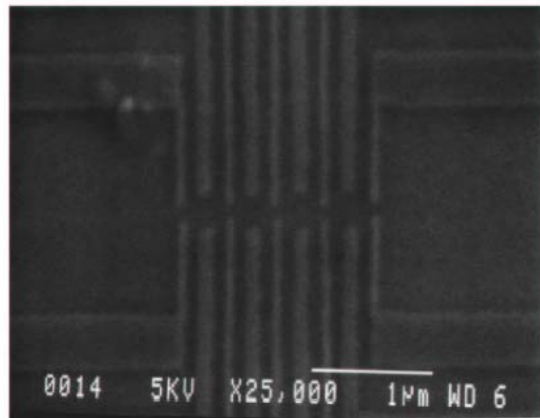
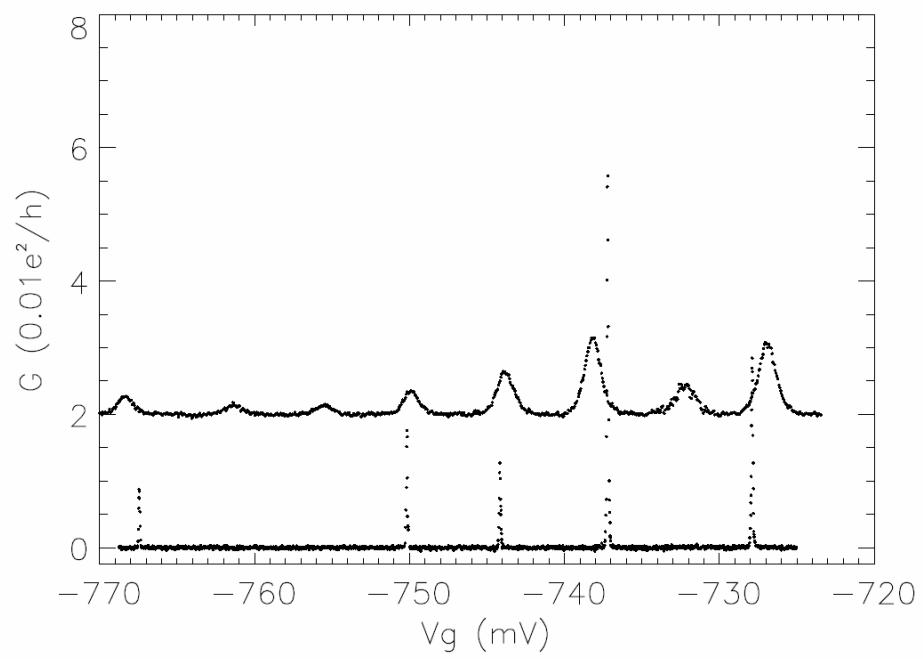


Semiconductor
Rings—Timp, Chang,
PRL 1987



Quantum Dot

- Single Electron Transistor—an electrometer sensitive to addition of a single electron, or to electric flux from 10^{-4} e
- Quantum levels inside the 0-dimensional system

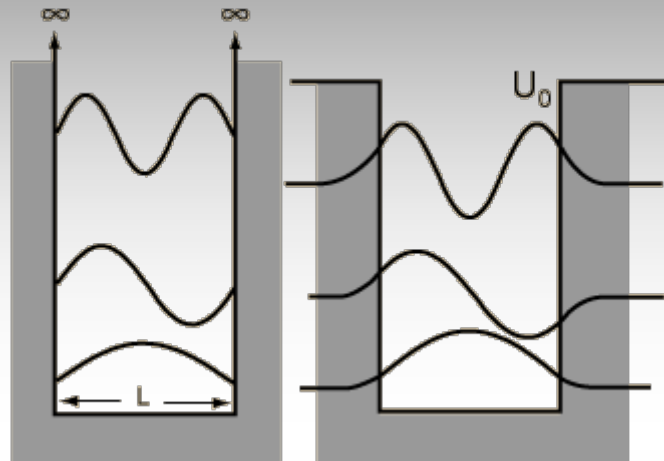
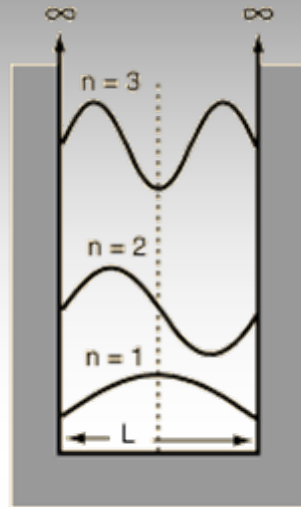


Key Concepts

- Size Quantization
- Quantum Coherence, Mesoscopics
- Phase Space in Reduced Dimensions
- Manybody effects

→ NOVEL PHYSICAL PROPERTIES

Size Quantization



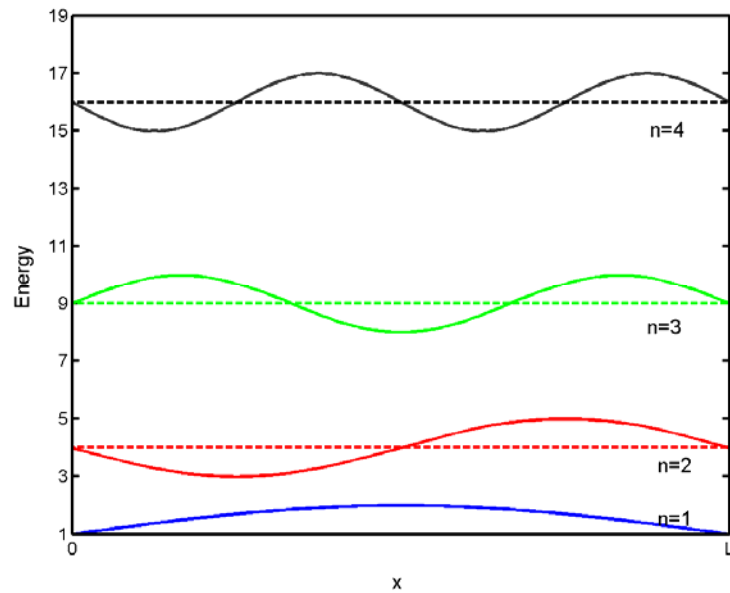
x = 0 at left wall of box.

$$\psi_n = \sqrt{\frac{2}{L}} \sin\left(\frac{n\pi x}{L}\right)$$

$$E_n = \frac{\hbar^2 \pi^2}{2mL^2} n^2$$

0-D: Particle in a 3D Box

For x, y, z, each—3D
confinement:



What is 0D, 1D, 2D? –3D, 2D, 1D confinement.

Coherence

- E.g. Laser speckle pattern—laser pointer on CD
- Holograms
- Aharonov-Bohm Effect
- Quantum Interference (Important for quantum computation)

FERMI SURFACE

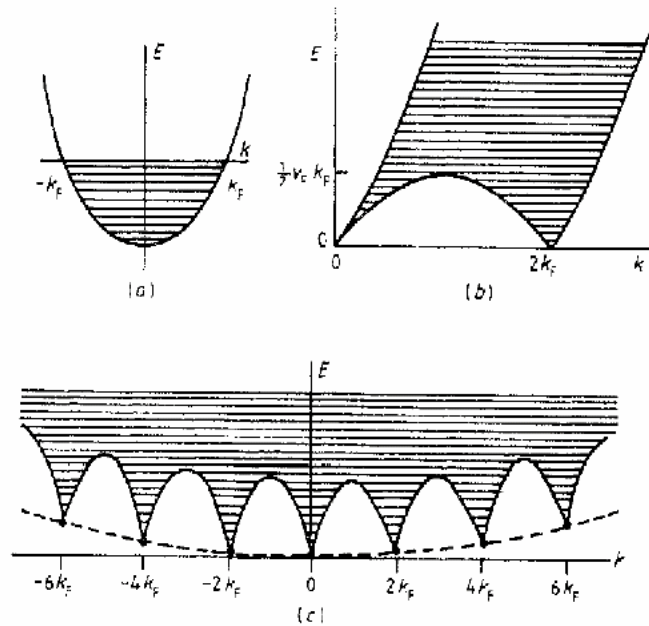
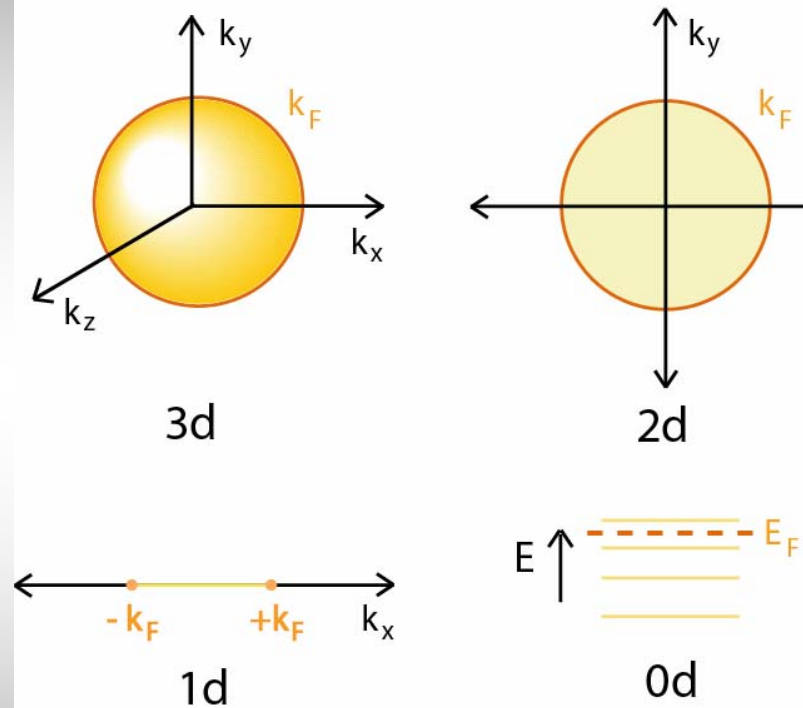


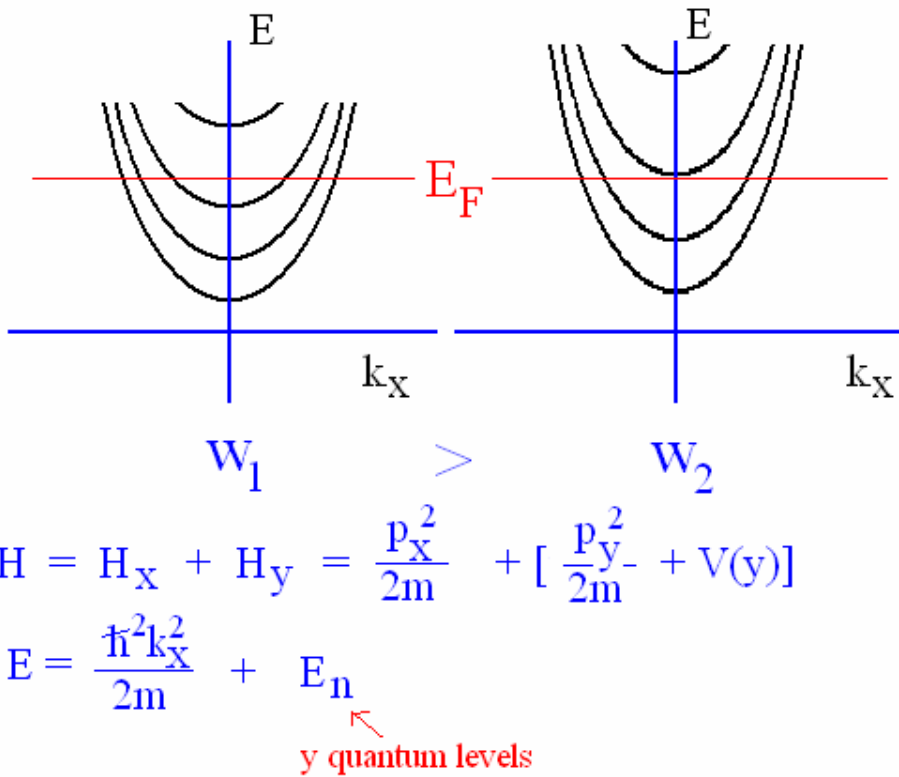
Figure 1. (a) Single-particle spectrum of the free Fermi gas in 1D; (b) Particle-hole spectrum; (c) full zero-charge (multiple particle-hole) excitation spectrum (energy differences $E(n) = 2\pi v_F n^2/L$ of extremal states at $k = 2nk_F$ greatly exaggerated).

F.D.M Haldane, J. Phys. C 14, 2585 (1981).

Outline

- Quantized Conductance in Quantum point contacts
- Aharonov Bohm Effect in mesoscopic rings
- 0-d: Quantum Dots
- Metallic nanowires and 1d superconductors

Quantized Conductance



$$\lambda = k_x / 2\pi \sim w$$

in a quasi-1-d channel

$$G = (e^2/h) \operatorname{Tr} t t^+$$

Ballistic Semiconductor Quantum Point Contact

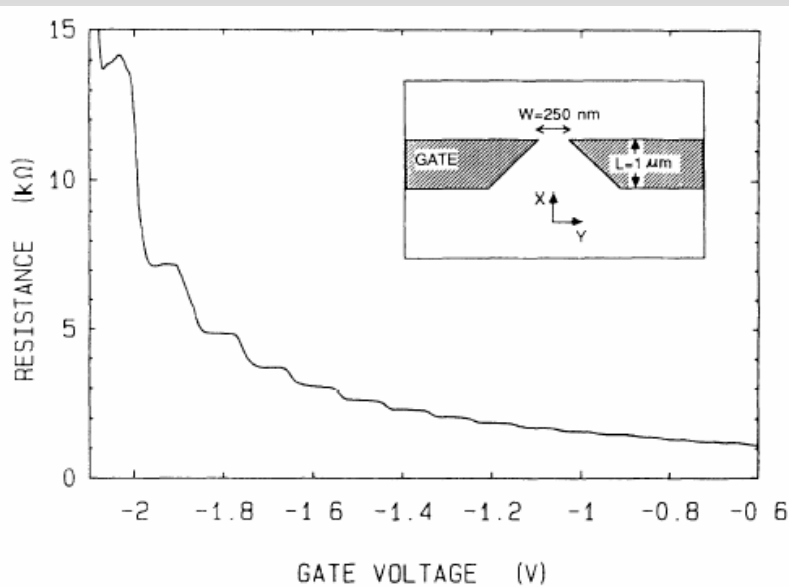


FIG. 1. Point-contact resistance as a function of gate voltage at 0.6 K. Inset: Point-contact layout.

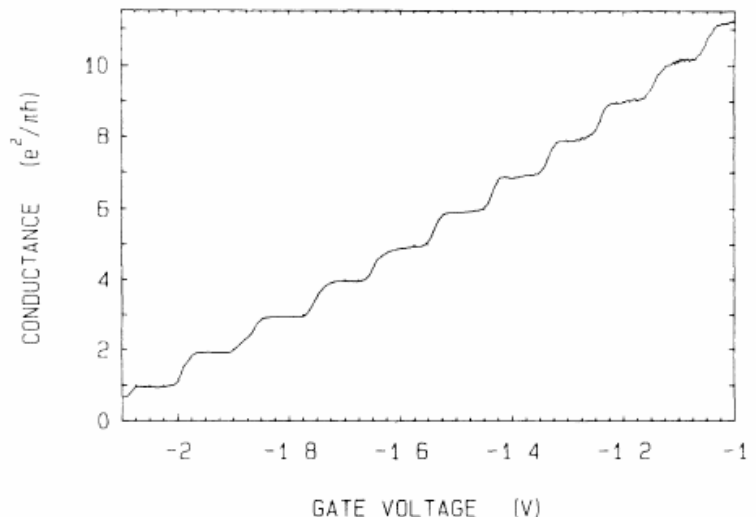


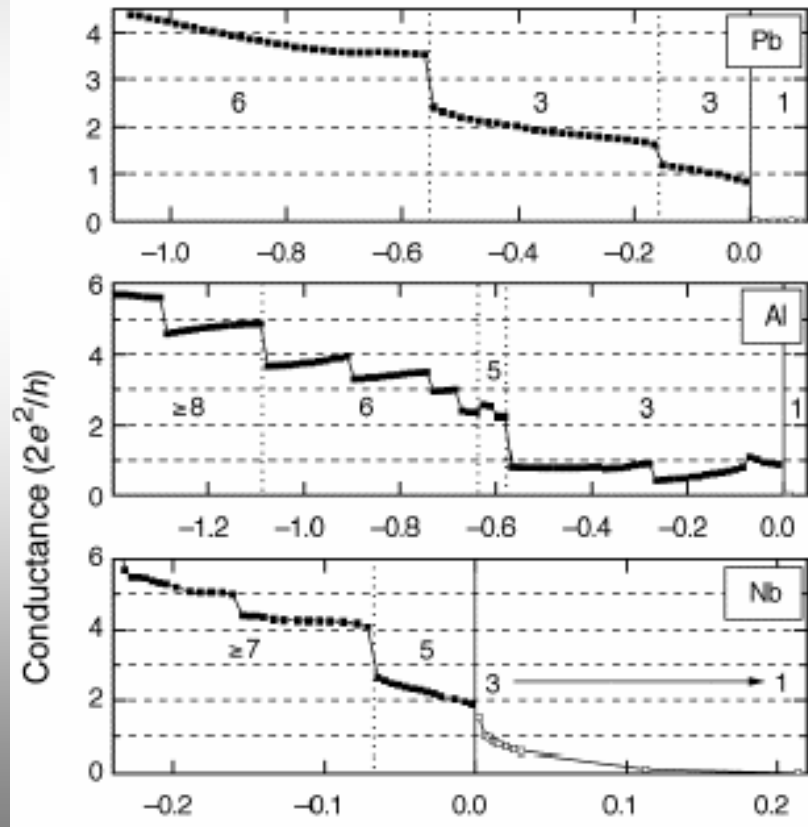
FIG. 2. Point-contact conductance as a function of gate voltage, obtained from the data of Fig. 1 after subtraction of the lead resistance. The conductance shows plateaus at multiples of $e^2/\pi\hbar$.

Quantized Conductance: $G = (e^2/h) \operatorname{Tr} t t^\dagger = (e^2/h) N$

B.J. van Wees et al. (1988) PRL; Wharam et al. (1988) J. Phys. C.

Atomic QPC

Scheer *et al.*, Nature 394, 154 (1998).



Evidence for Saturation of Channel Transmission from Conductance Fluctuations in Atomic-Size Point Contacts

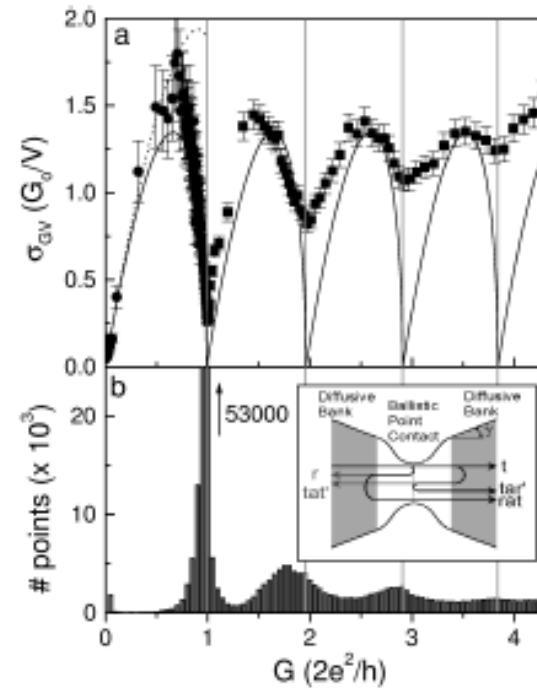
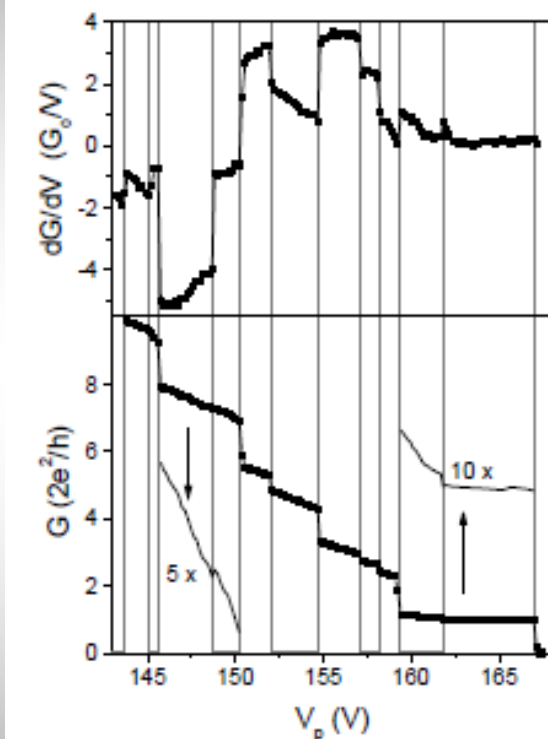
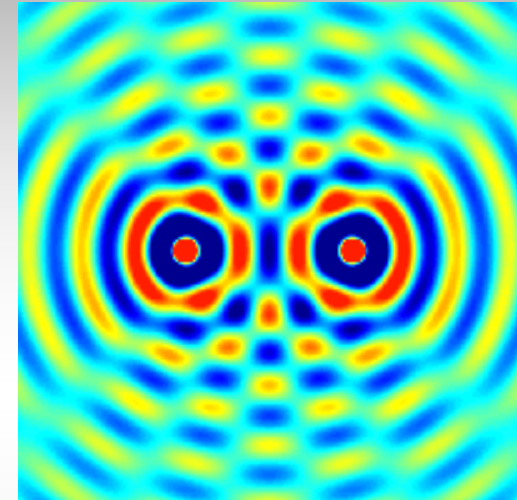
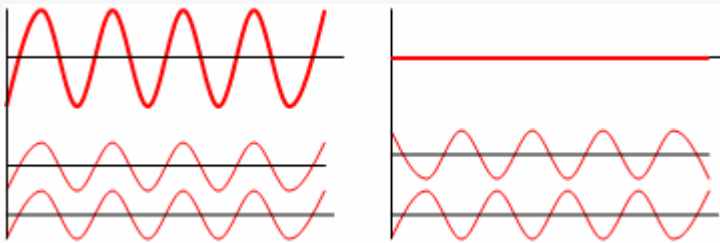


FIG. 3. (a) Standard deviation of the voltage dependence of the conductance versus conductance for 3500 curves. The

Au break junctions: Ludolph et al., PRL 1999.

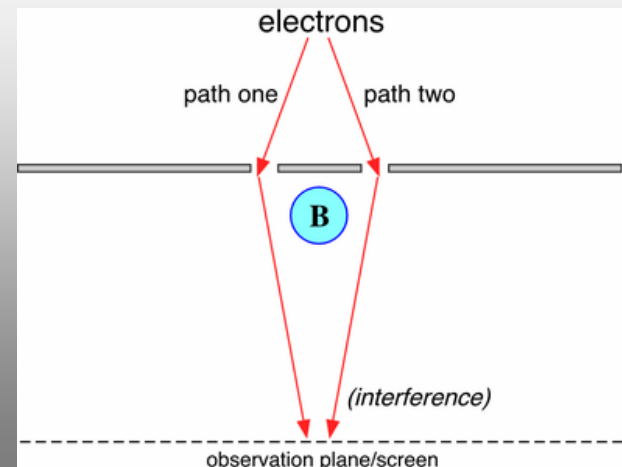
Aharono-Bohm Effect

Wave Interference

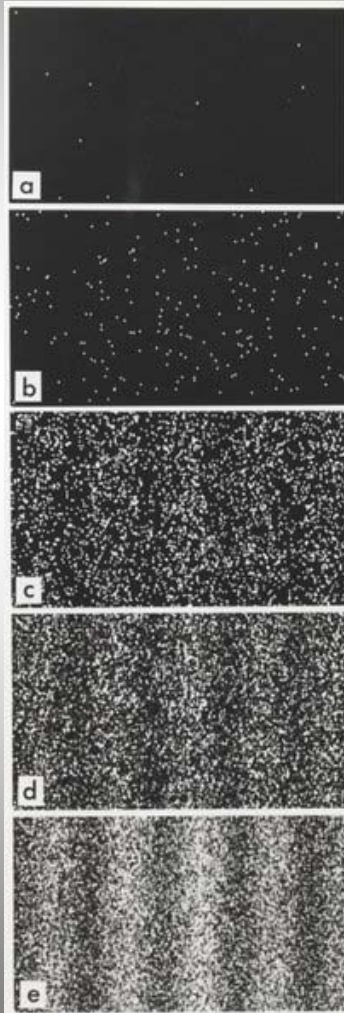


$$I = I_o \cos^2(\Delta\phi/2)$$

$$\varphi = \frac{q}{\hbar} \int_P \mathbf{A} \cdot d\mathbf{x},$$



Electron Interference



$$H = \frac{1}{2m}(\mathbf{p} - q\mathbf{A})^2$$

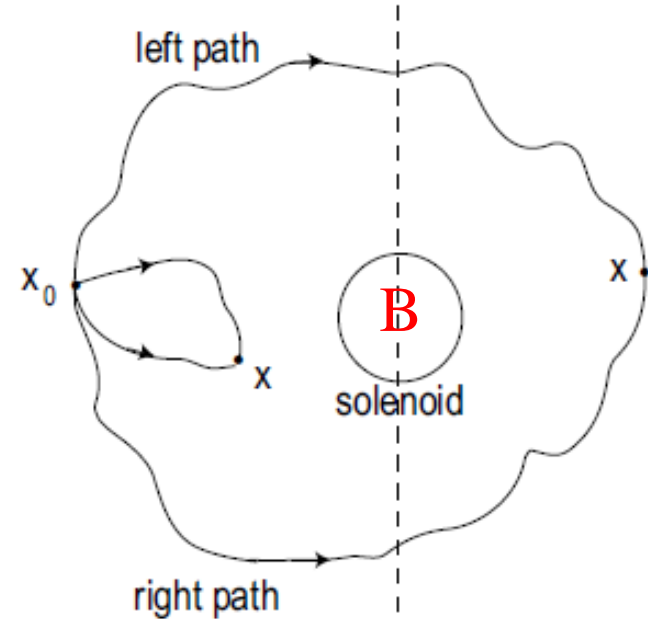
$$\psi_{\Phi}(\mathbf{x}, t) = \psi_{\ell}(\mathbf{x}, t)e^{iqs_{\ell}(\mathbf{x})} + \psi_r(\mathbf{x}, t)e^{iqs_r(\mathbf{x})} ; \mathbf{q} = 2\pi\mathbf{e}/\mathbf{h}$$

$$s_{\ell}(\mathbf{x}) \equiv \int_{\mathbf{x}_i}^{\mathbf{x}} \mathbf{A}(\mathbf{x}') \cdot d\mathbf{x}',$$

left path

$$s_r(\mathbf{x}) \equiv \int_{\mathbf{x}_i}^{\mathbf{x}} \mathbf{A}(\mathbf{x}') \cdot d\mathbf{x}'$$

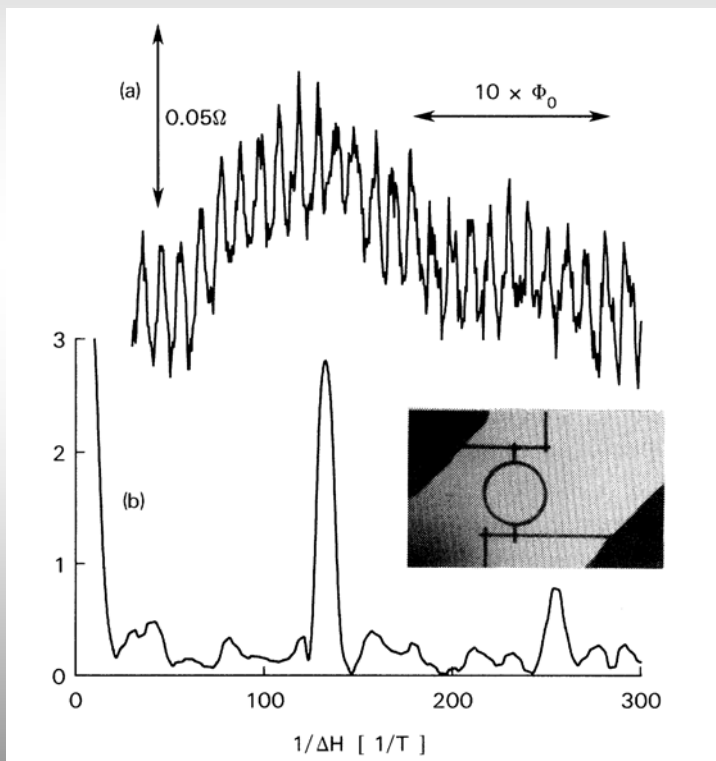
right path



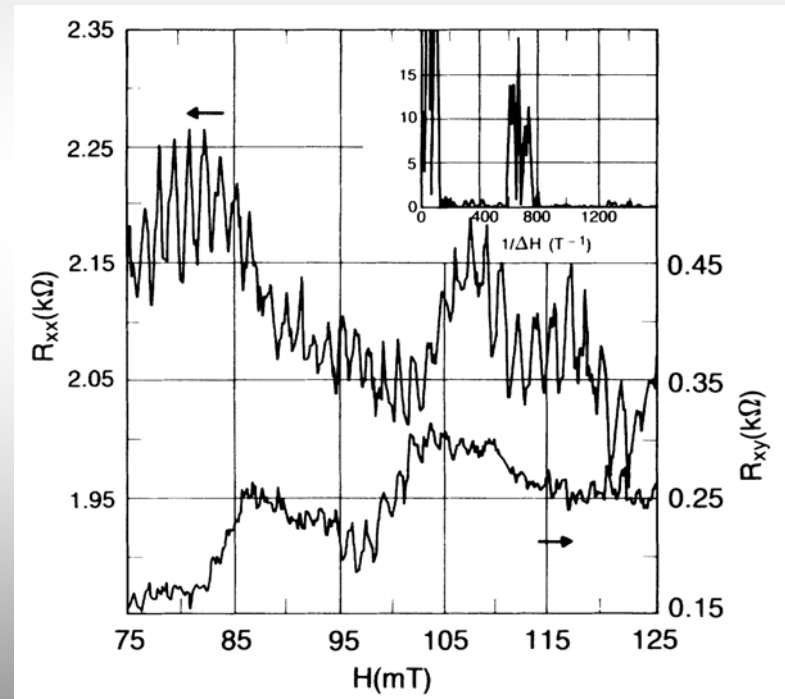
$$\oint_{\text{-left path}} \mathbf{A}(\mathbf{x}') \cdot d\mathbf{x}' = \begin{cases} 0 & \mathbf{x} \text{ in front of solenoid} \\ \Phi & \mathbf{x} \text{ behind solenoid.} \end{cases} = \mathbf{B} \times (\text{Area})$$

$\oint_{\text{+right path}}$

Metallic Rings— R.A. Webb, PRL 1985



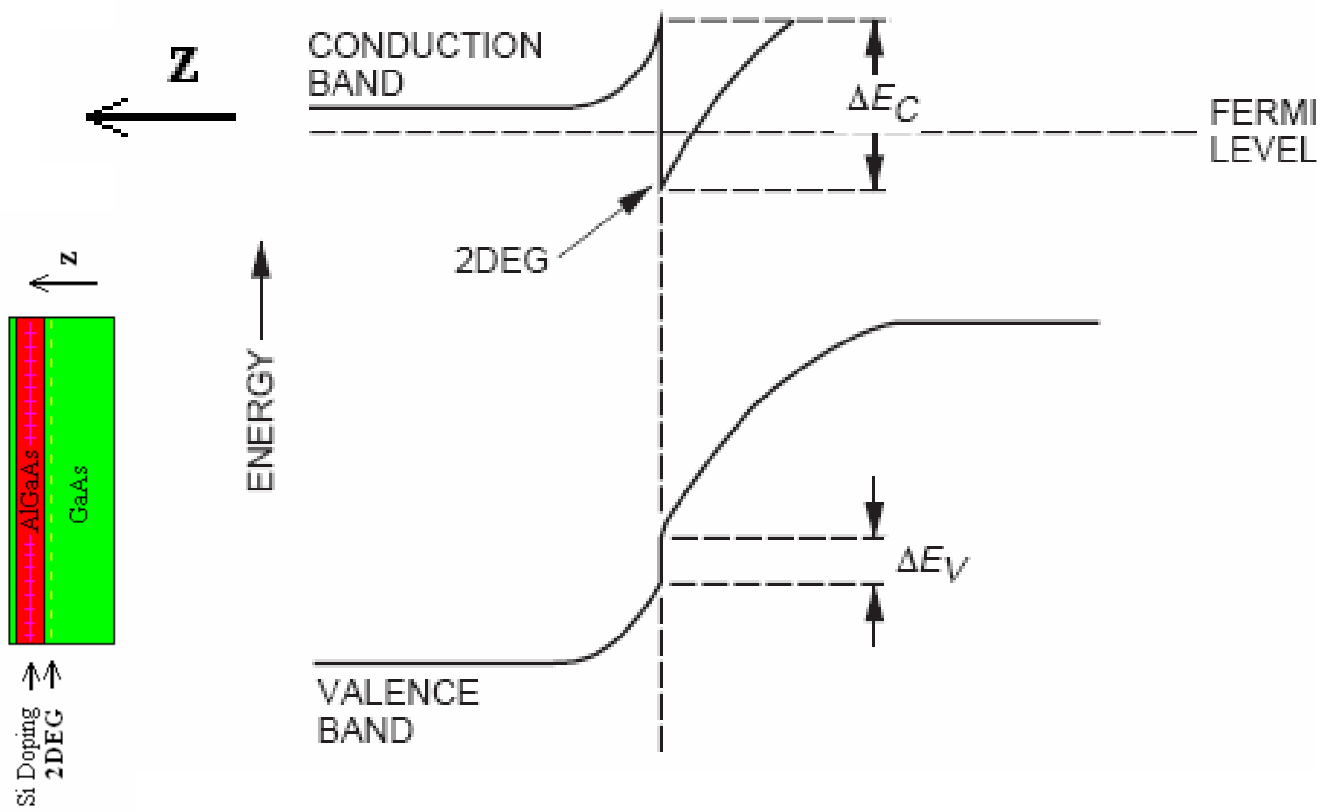
Semiconductor Rings—Timp, Chang, PRL 1987

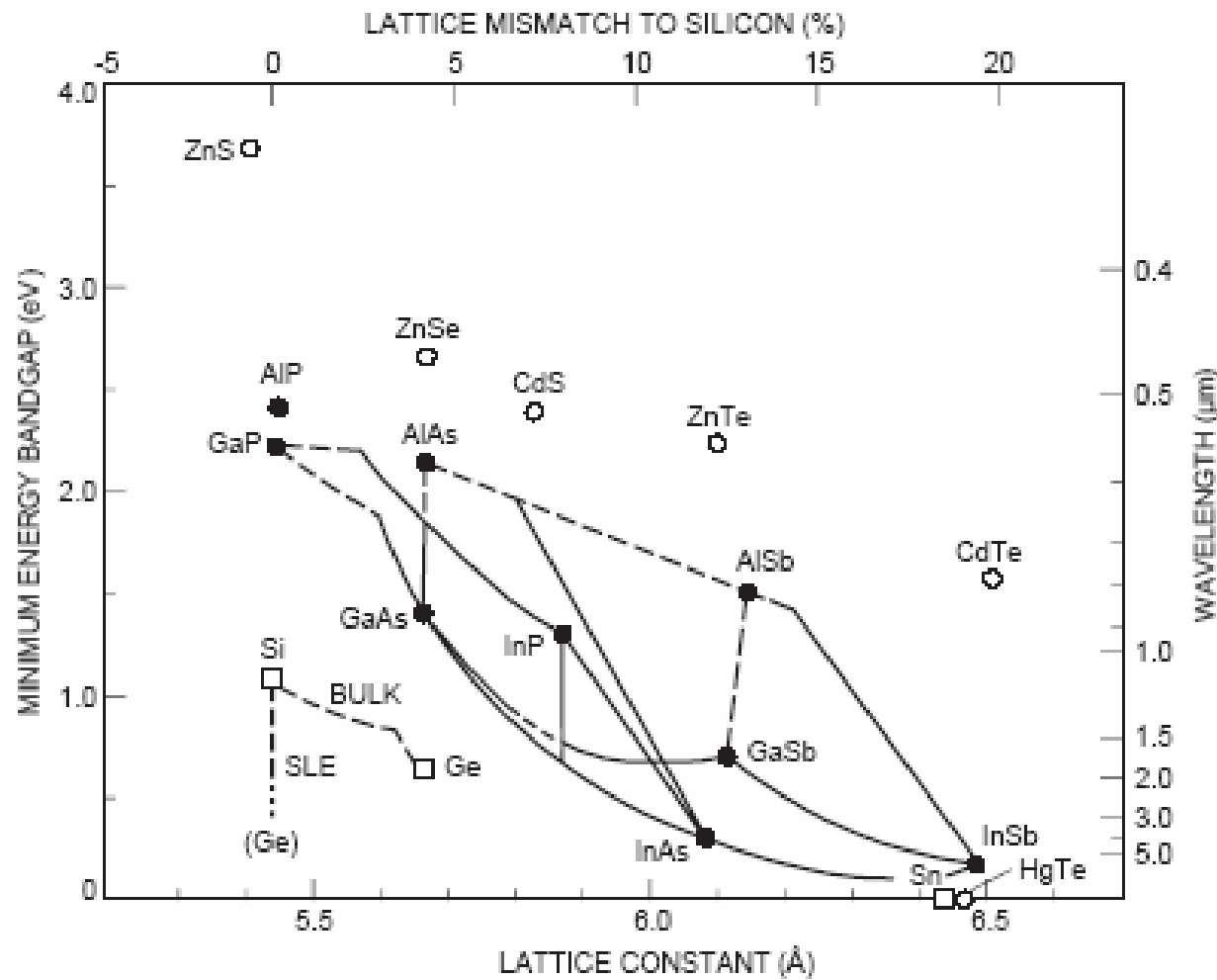


Systems

- Semiconductor—2DEG, 1DEG, Quantum Dots
- Metallic—Nanowires and rings, Quantum Dots,
- Molecular and atomic systems
- New Materials: e.g. Carbon nanotubes, graphene sheets

2-Dimensional Electron Gas in GaAs-AlGaAs Heterostructure





The Hall Effect

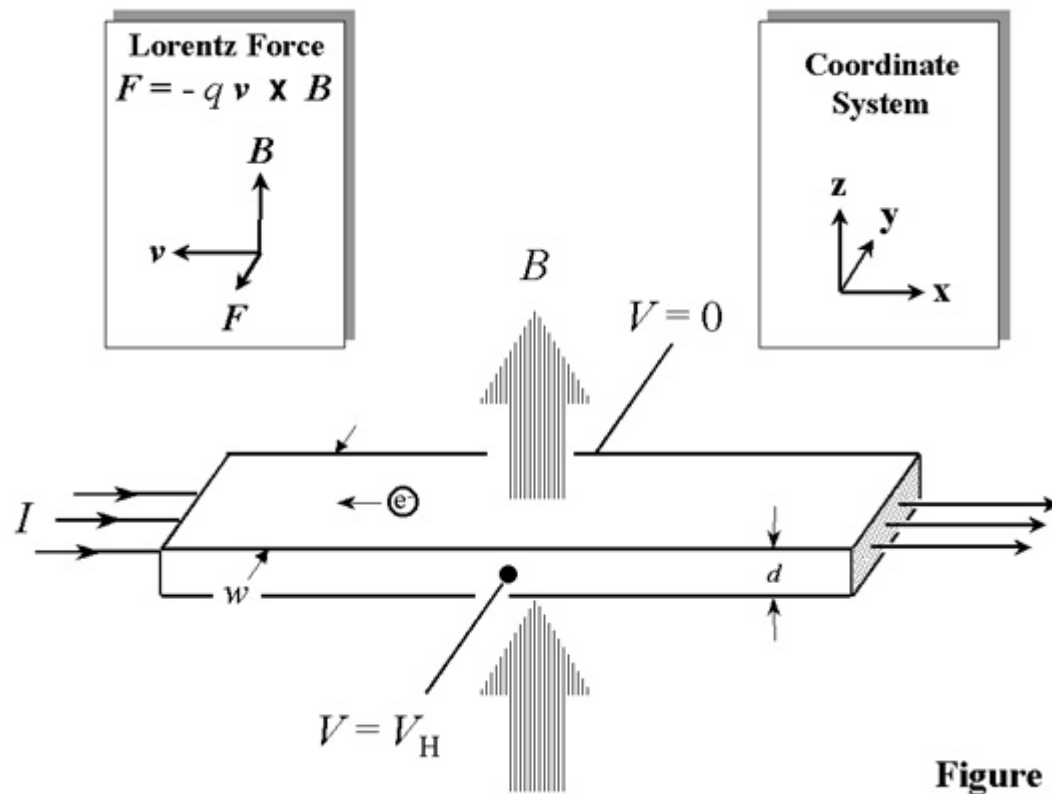


Figure 1

Classical Drude Conductivity

$$\mathbf{v}_d = -e\mathbf{E}\tau/m \quad (1)$$

$$\mathbf{j} = -nev_d = \sigma_0 \mathbf{E} \quad \sigma_0 = ne^2\tau/m \quad (2)$$

$$\begin{aligned} \mathbf{j} &= \sigma \cdot \mathbf{E} \\ \mathbf{E} &= \rho \cdot \mathbf{j} \end{aligned} \quad \sigma = \begin{pmatrix} \sigma_{xx} & \sigma_{xy} \\ \sigma_{yx} & \sigma_{yy} \end{pmatrix}, \quad \rho = \begin{pmatrix} \rho_{xx} & \rho_{xy} \\ \rho_{yx} & \rho_{yy} \end{pmatrix} \quad (4)$$

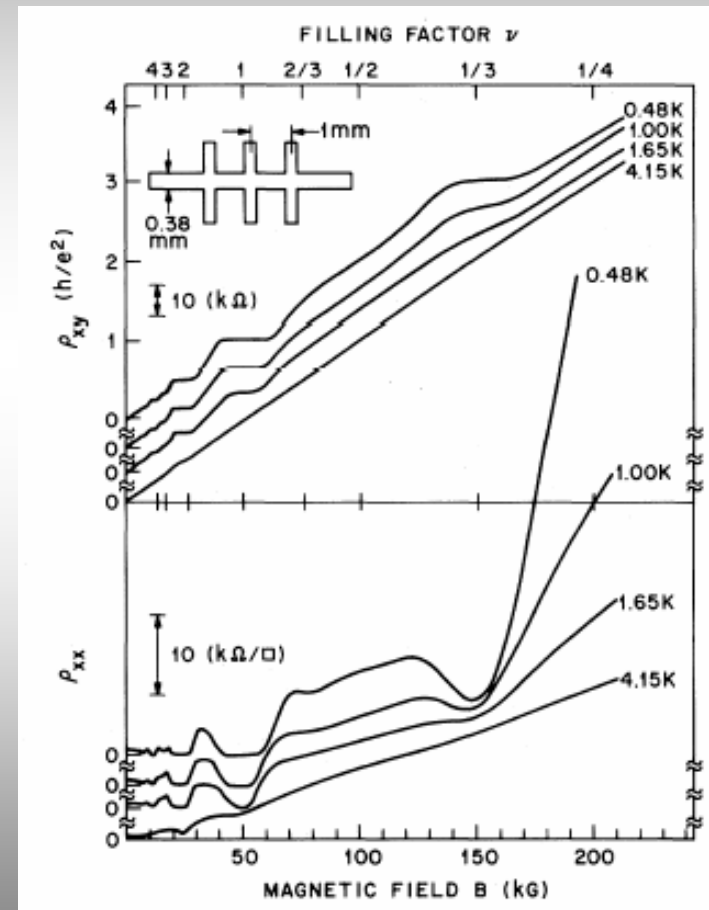
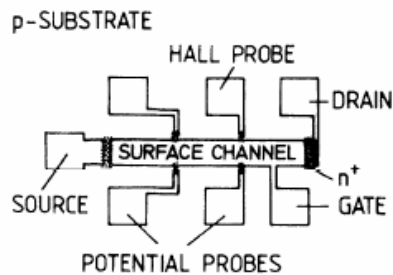
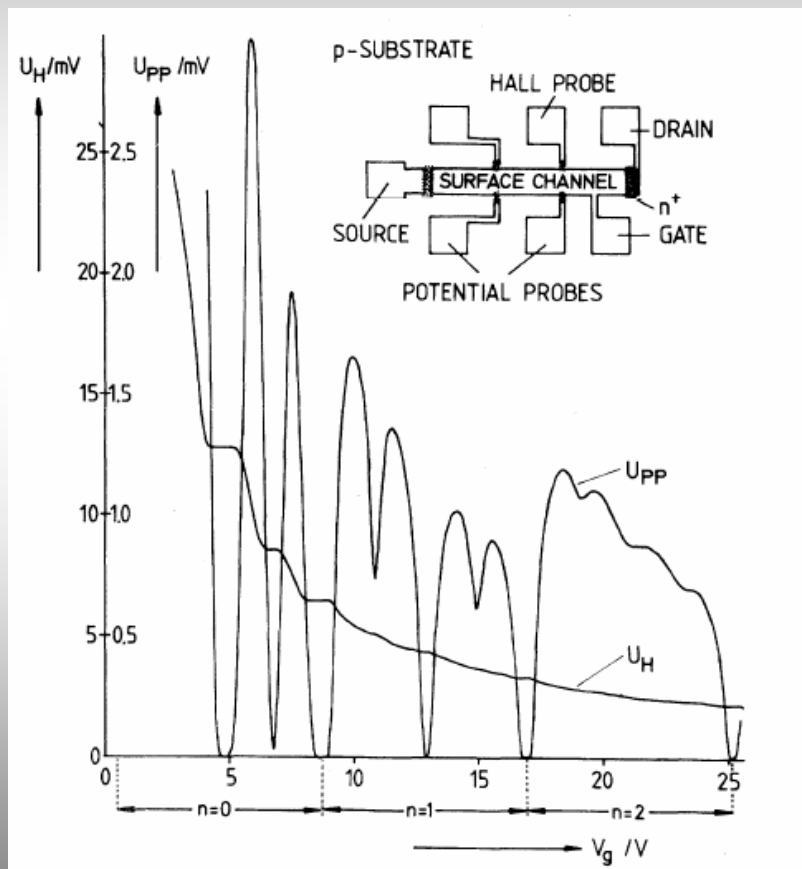
$$\mathbf{v}_d = -e \left(\mathbf{E} + \frac{\mathbf{v}_d \times \mathbf{B}}{c} \right) \frac{\tau}{m} \quad (5)$$

$$\begin{aligned} \sigma_0 E_x &= \omega_c \tau j_y + j_x \\ \sigma_0 E_y &= -\omega_c \tau j_x + j_y \end{aligned} \quad \omega_c = \frac{eB}{mc} \quad (6)$$

$$\rho_{xx} = \rho_{yy} = 1/\sigma_0, \quad \rho_{xy} = -\rho_{yx} = \omega_c \tau / \sigma_0$$

$$\sigma_{xx} = \sigma_{yy} = \frac{\sigma_0}{1 + (\omega_c \tau)^2}, \quad \sigma_{xy} = -\sigma_{yx} = \frac{-\sigma_0 \omega_c \tau}{1 + (\omega_c \tau)^2}$$

2DEG-Quantized Hall Effect

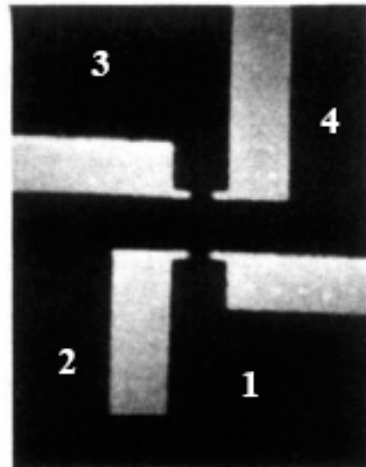


Von Klitzing, PRL 1980

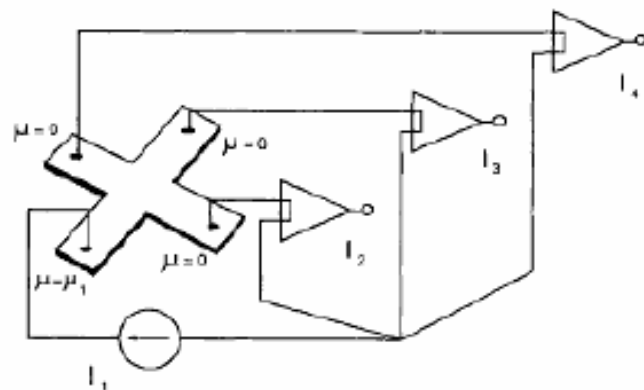
Tsui, Stormer, PRL 1982

Reciprocity—Buttiker, Landauer

Cross geometry



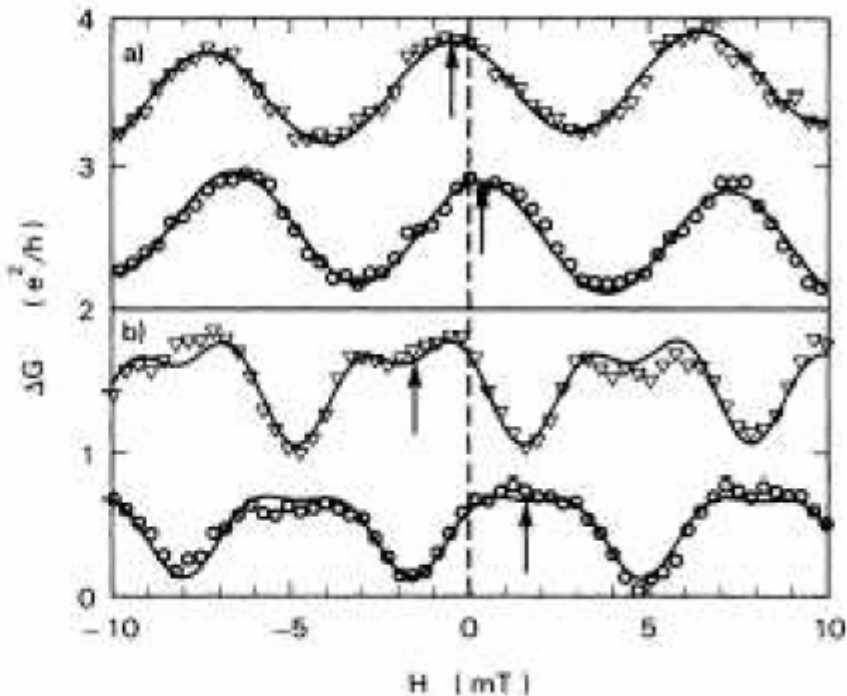
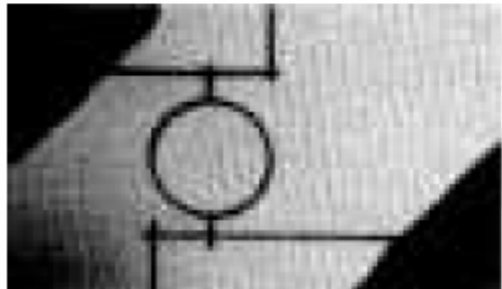
Shephard *et al.*, PRB **46**, 9648 (1992).



- Usual GaAs 2deg + Au gates.

Reciprocity: Benoit et al.

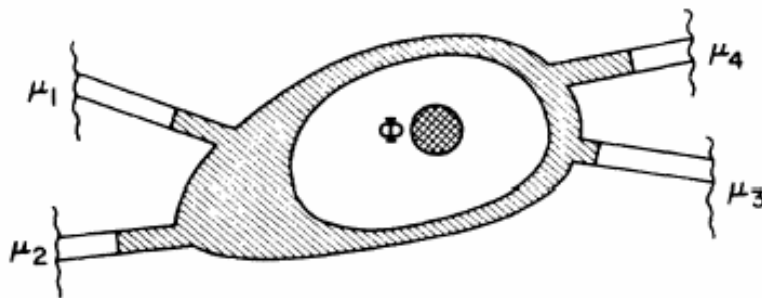
Benoit, Washburn, Umbach, Laibowitz, Webb, PRL 57, 1765 (1986)



Four-Terminal Phase-Coherent Conductance

M. Büttiker

IBM Thomas J. Watson Research Center, Yorktown Heights, New York 10598



$$I_i = \frac{e}{h} \left[(1 - R_{ii})\mu_i - \sum_{j \neq i} T_{ij}\mu_j \right]$$

$$\mathcal{R}_{mn,kl} = (h/e^2)(T_{km}T_{ln} - T_{kn}T_{lm})/D$$

$$R_{ii}(\Phi) = R_{ii}(-\Phi), \quad T_{ij}(\Phi) = T_{ji}(-\Phi).$$

Fermi-Dirac; Fermi Level

$$f(E) = \frac{1}{e^{(E - E_F)/kT} + 1}$$

$$E = \frac{p^2}{2m} = \left(\frac{\hbar}{\lambda}\right)^2 \frac{1}{2m} = \left(\frac{\hbar}{2\pi} \frac{2\pi}{\lambda}\right)^2 \frac{1}{2m} = \frac{(\hbar k)^2}{2m}$$

$$k = \frac{\sqrt{2mE}}{\hbar} \quad k = n(2\pi/L); L = \text{size of system}$$

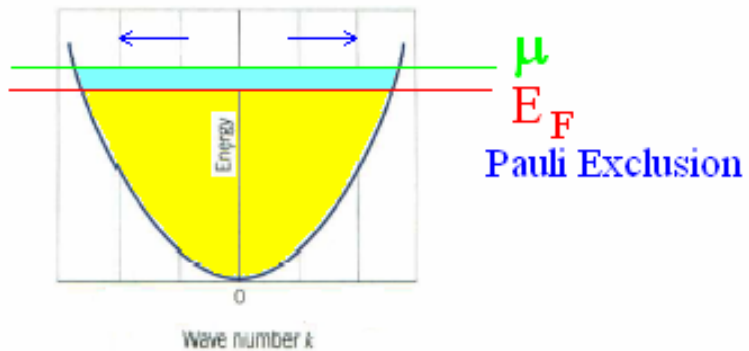
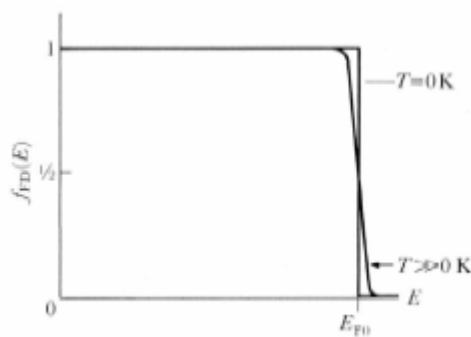


FIGURE 11.25 The parabolic relationship between energy and wave number for a free particle.

as a function of differences of voltages, $V_i = \mu_i/e$,

$$I_1 = \alpha_{11}(V_1 - V_3) - \alpha_{12}(V_2 - V_4), \quad (3a)$$

$$I_2 = -\alpha_{21}(V_1 - V_3) + \alpha_{22}(V_2 - V_4). \quad (3b)$$

I find the following expressions for the conductances of Eq. (3):

$$\begin{aligned} \alpha_{11} &= (e^2/h)[(1-R_{11})S \\ &\quad - (T_{14}+T_{12})(T_{41}+T_{21})]/S, \end{aligned} \quad (4a)$$

$$\alpha_{12} = (e^2/h)(T_{12}T_{34} - T_{14}T_{32})/S, \quad (4b)$$

$$\alpha_{21} = (e^2/h)(T_{21}T_{43} - T_{23}T_{41})/S, \quad (4c)$$

$$\begin{aligned} \alpha_{22} &= (e^2/h)[(1-R_{22})S \\ &\quad - (T_{21}+T_{23})(T_{32}+T_{12})]/S, \end{aligned} \quad (4d)$$

where

$$\begin{aligned} S &= T_{12} + T_{14} + T_{32} + T_{34} \\ &= T_{21} + T_{41} + T_{23} + T_{43}. \end{aligned} \quad (5)$$

Buttiker

$$\mathcal{R}_{13,24} = (V_2 - V_4)/I_1 = \alpha_{21}/(\alpha_{11}\alpha_{22} - \alpha_{12}\alpha_{21}).$$

The Hall Effect

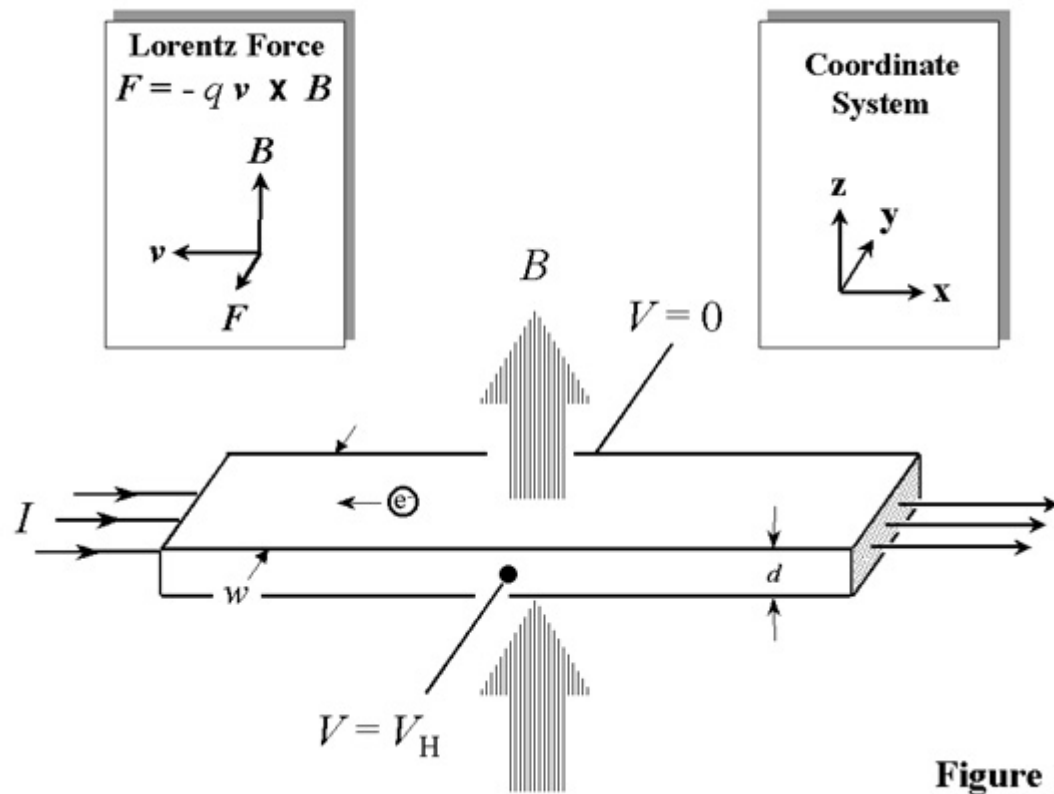


Figure 1

Classical Drude Conductivity

$$\mathbf{v}_d = -e\mathbf{E}\tau/m \quad (1)$$

$$\mathbf{j} = -nev_d = \sigma_0 \mathbf{E} \quad \sigma_0 = ne^2\tau/m \quad (2)$$

$$\begin{aligned} \mathbf{j} &= \sigma \cdot \mathbf{E} \\ \mathbf{E} &= \rho \cdot \mathbf{j} \end{aligned} \quad \sigma = \begin{pmatrix} \sigma_{xx} & \sigma_{xy} \\ \sigma_{yx} & \sigma_{yy} \end{pmatrix}, \quad \rho = \begin{pmatrix} \rho_{xx} & \rho_{xy} \\ \rho_{yx} & \rho_{yy} \end{pmatrix} \quad (4)$$

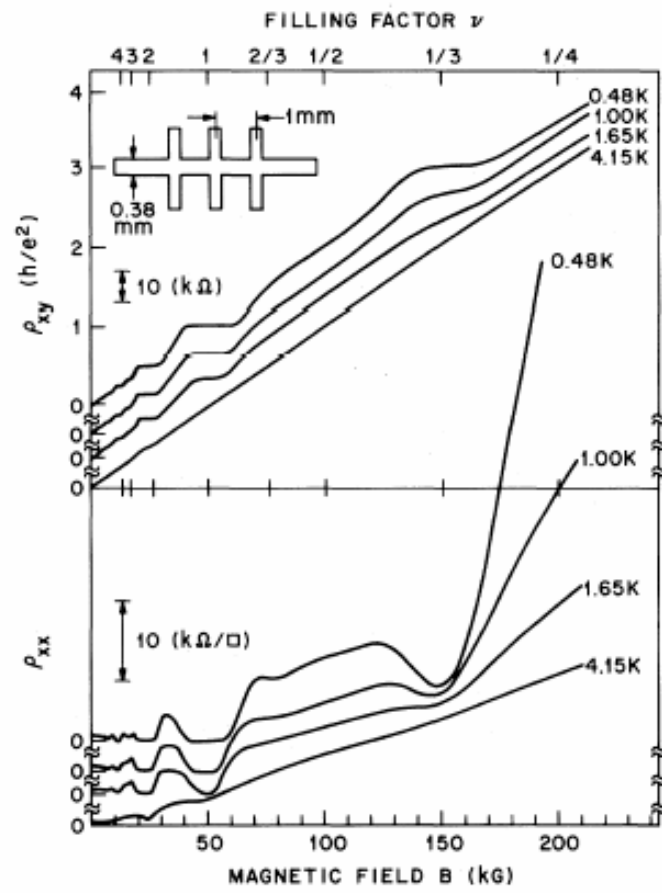
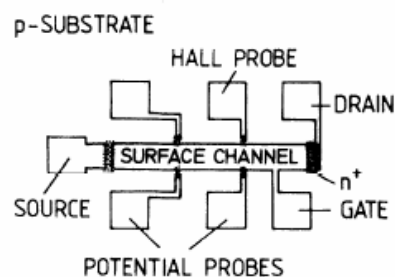
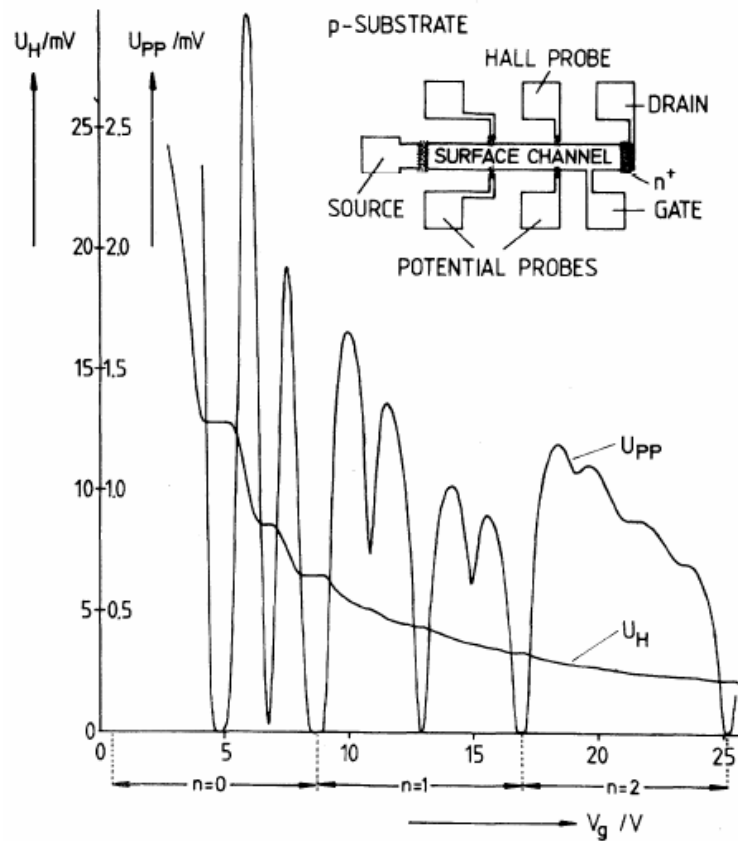
$$\mathbf{v}_d = -e \left(\mathbf{E} + \frac{\mathbf{v}_d \times \mathbf{B}}{c} \right) \frac{\tau}{m} \quad (5)$$

$$\begin{aligned} \sigma_0 E_x &= \omega_c \tau j_y + j_x \\ \sigma_0 E_y &= -\omega_c \tau j_x + j_y \end{aligned} \quad \omega_c = \frac{eB}{mc} \quad (6)$$

$$\rho_{xx} = \rho_{yy} = 1/\sigma_0, \quad \rho_{xy} = -\rho_{yx} = \omega_c \tau / \sigma_0$$

$$\sigma_{xx} = \sigma_{yy} = \frac{\sigma_0}{1 + (\omega_c \tau)^2}, \quad \sigma_{xy} = -\sigma_{yx} = \frac{-\sigma_0 \omega_c \tau}{1 + (\omega_c \tau)^2}$$

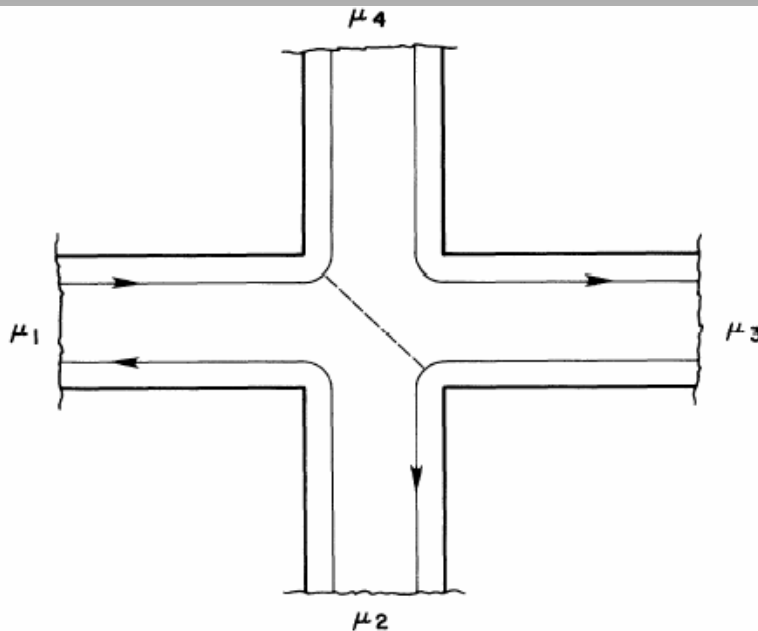
2DEG-Quantized Hall Effect



Von Klitzing, PRL 1980

Tsui, Stormer, PRL 1982

Buttiker Formalism

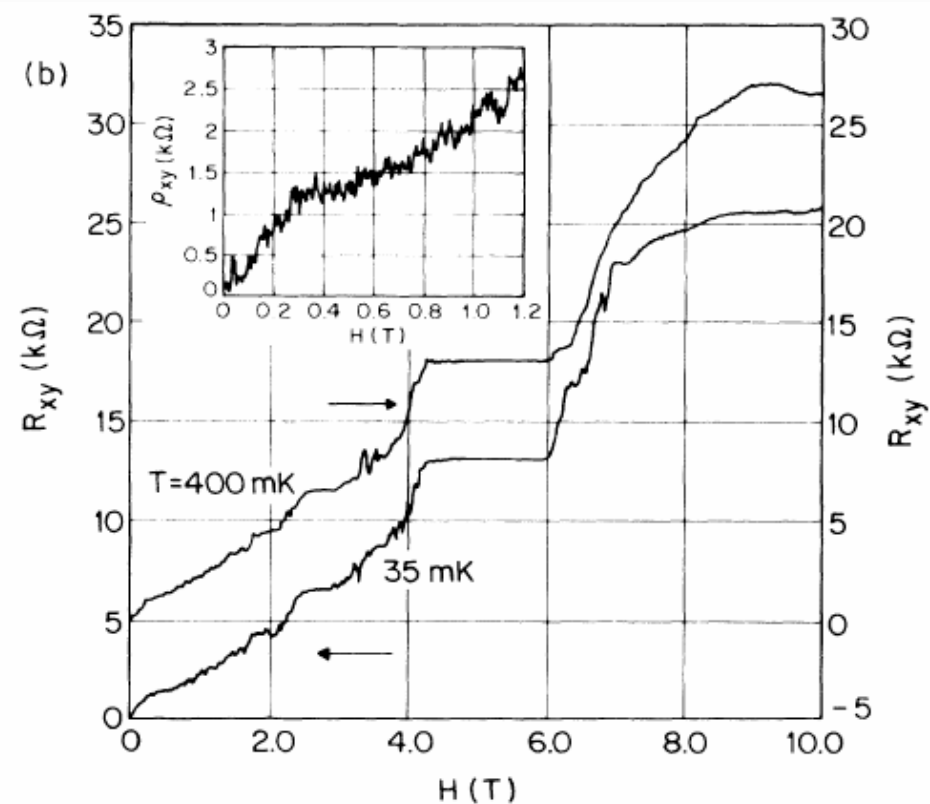


Buttiker, PRL 1989

Timp, Chang, PRL 1987

Refs. 2 and 6.) We have $T_{12} = T_{34} = N$, and $T_{21} = T_{43} \equiv \mathcal{T}$, $T_{23} = T_{41} = N - \mathcal{T}$. Using Eq. (1) we find a Hall resistance

$$\mathcal{R}_H = \mathcal{R}_{13,42} = \frac{h}{e^2} \left(\frac{1}{N} - \frac{\mathcal{T}}{N(N-\mathcal{T})} \right). \quad (2)$$



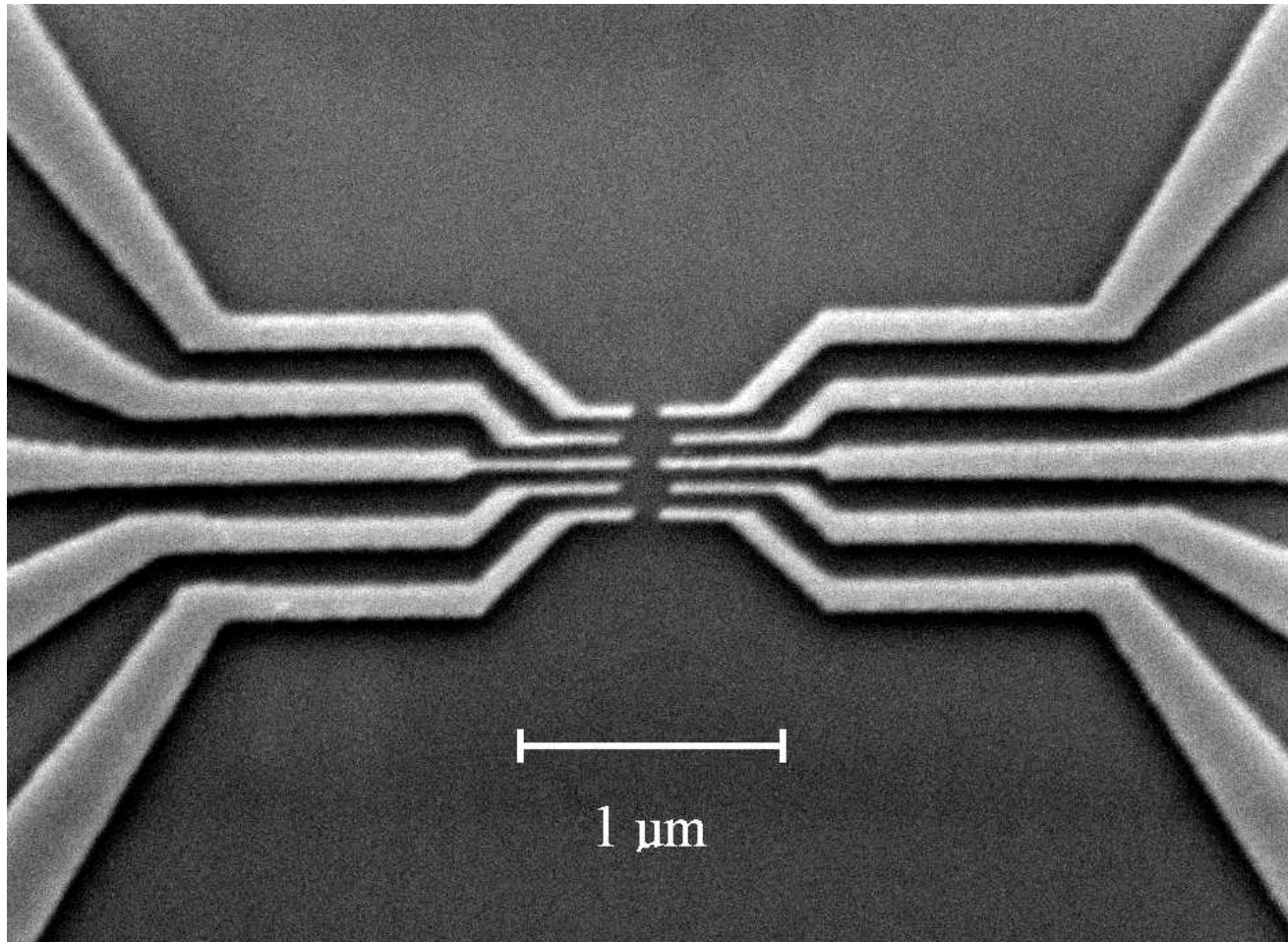
KONDO EFFECT AND SPIN - ENTANGLEMENT IN DOUBLE QUANTUM DOTS

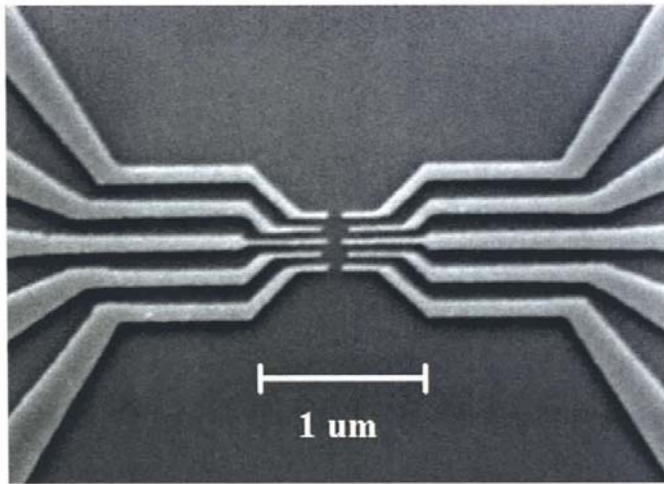
ALBERT M. CHANG

Department of Physics

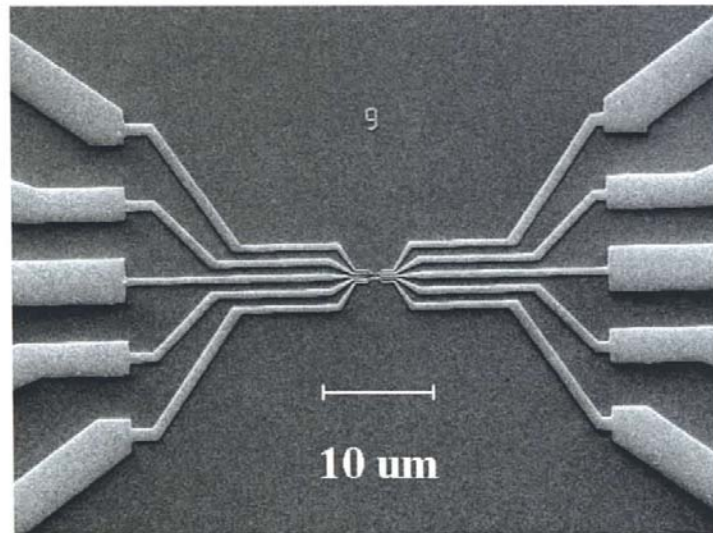
Duke University, Durham, NC 27708

Double Quantum Dot Molecule



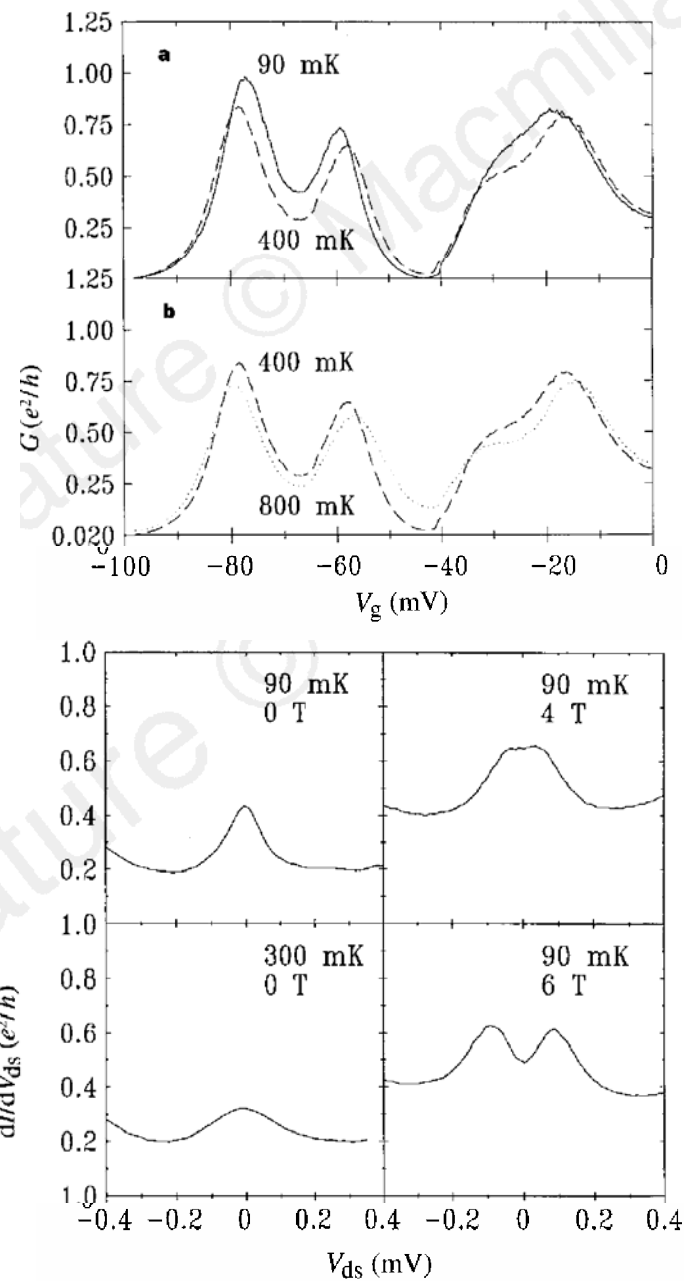
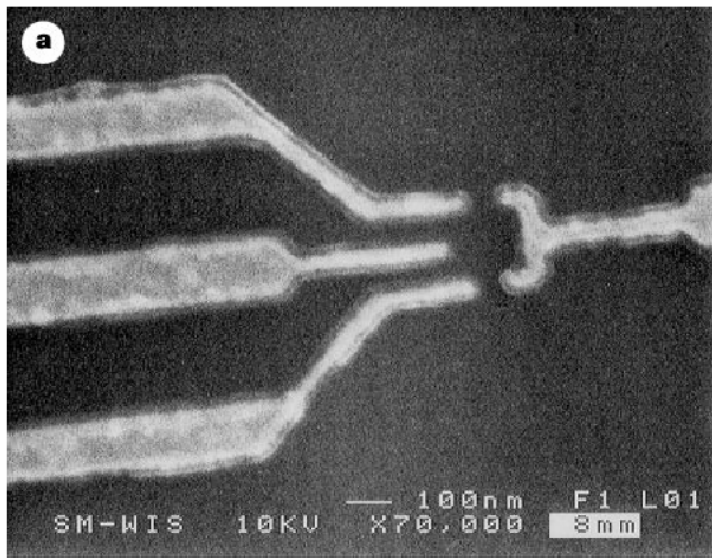


The size is 180 nm. Designed for 'the Kondo effect in artificial molecules'.

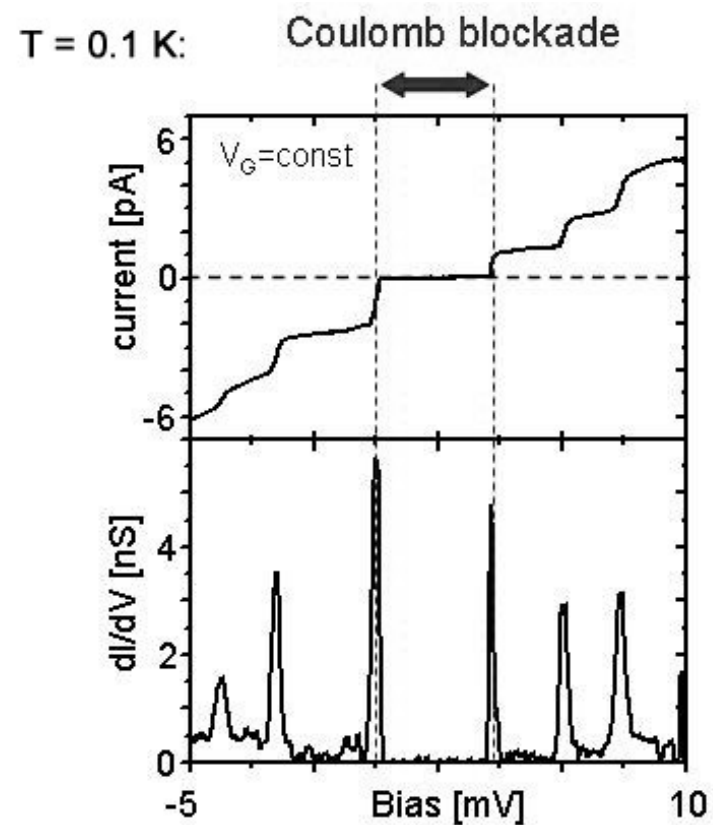
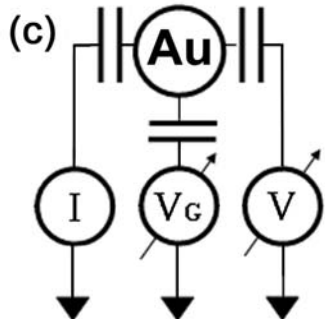
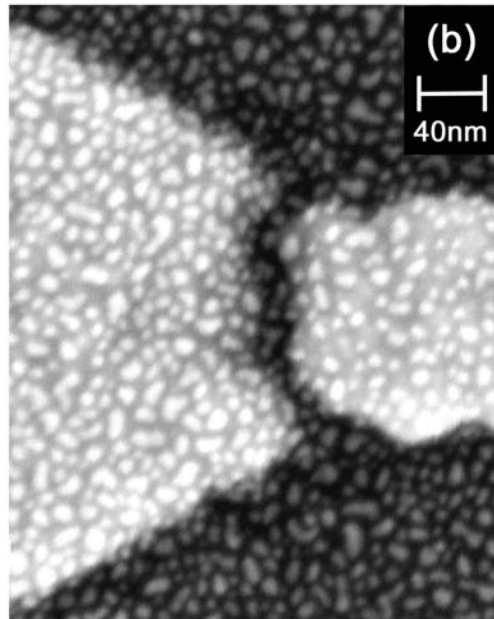
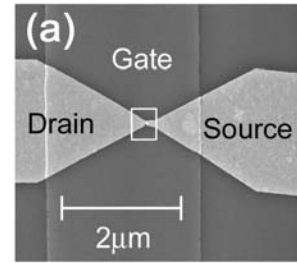


Bigger picture of the above device showing outer fan-out.

**D. Goldhaber-Gordon,
M.A. Kastner et al.,
Nature 391, 156-159 (1998).**

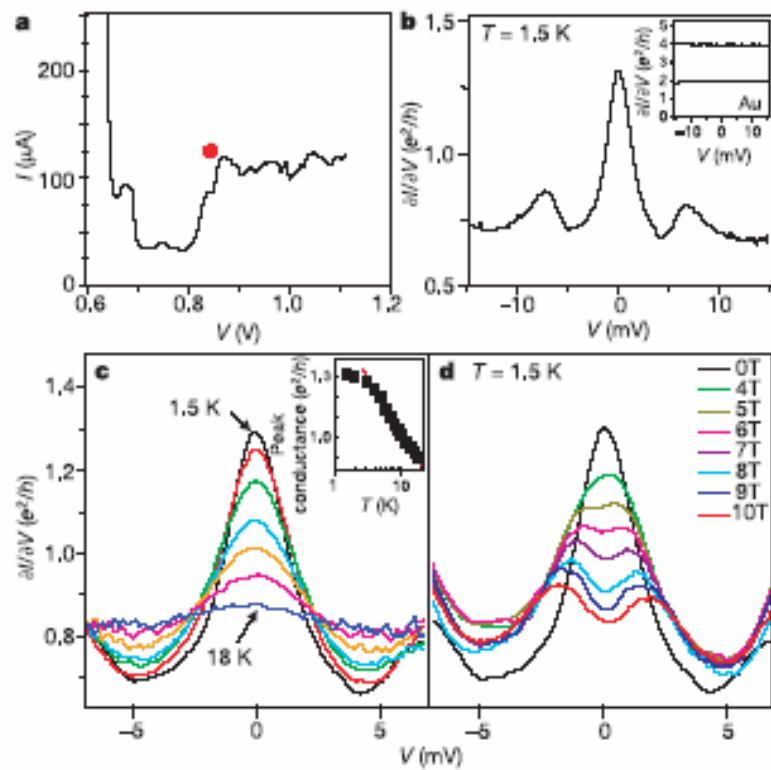
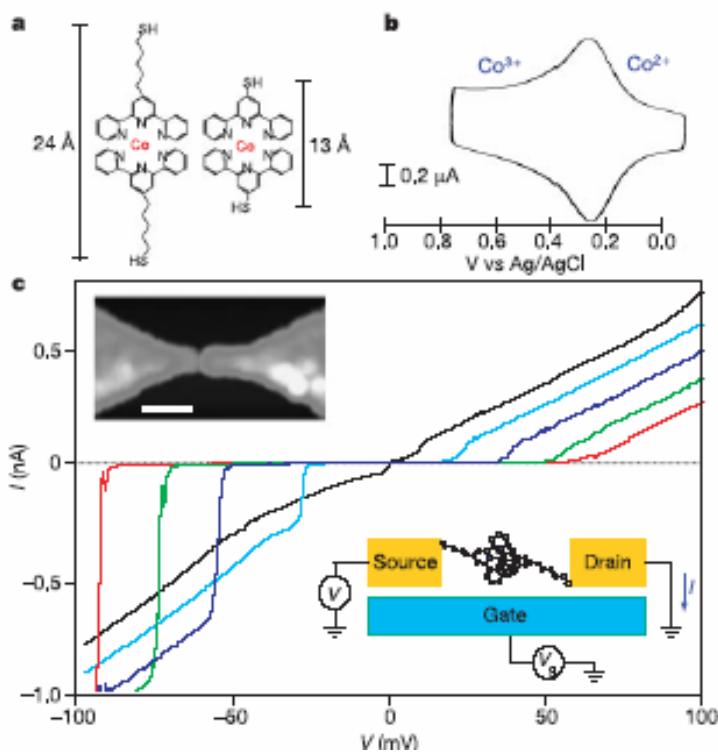


Gold Nanoparticles



Ralph (Cornell)

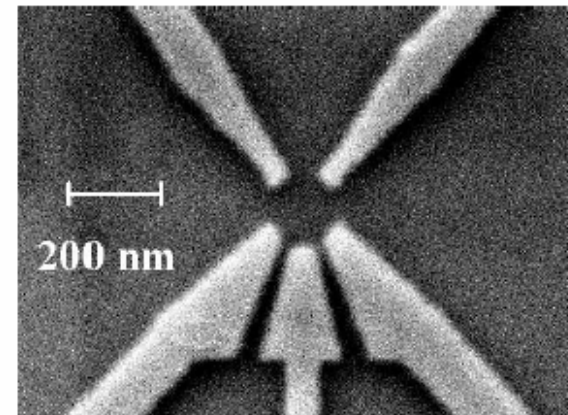
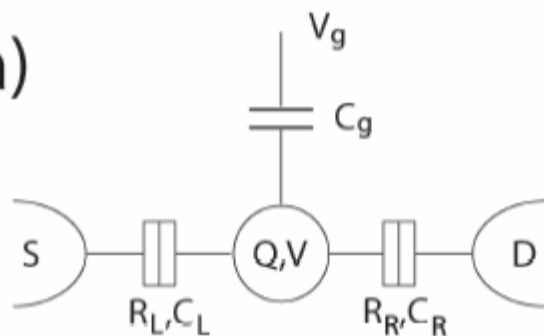
Single Atom Transistor



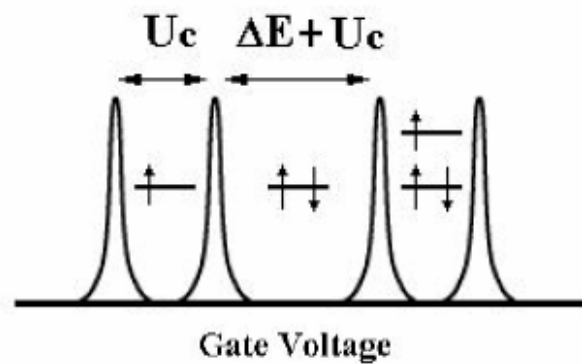
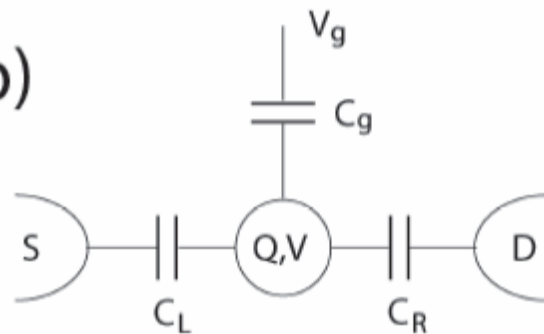
McEuen, Ralph, et al., Nature 2002.

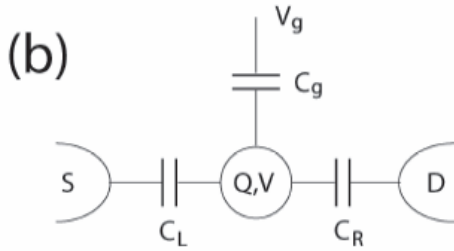
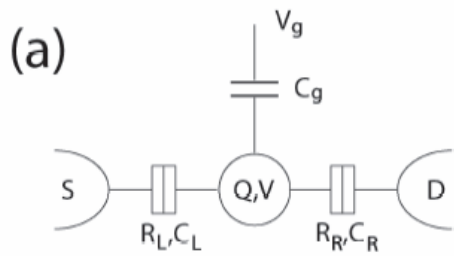
Quantum Dots

(a)



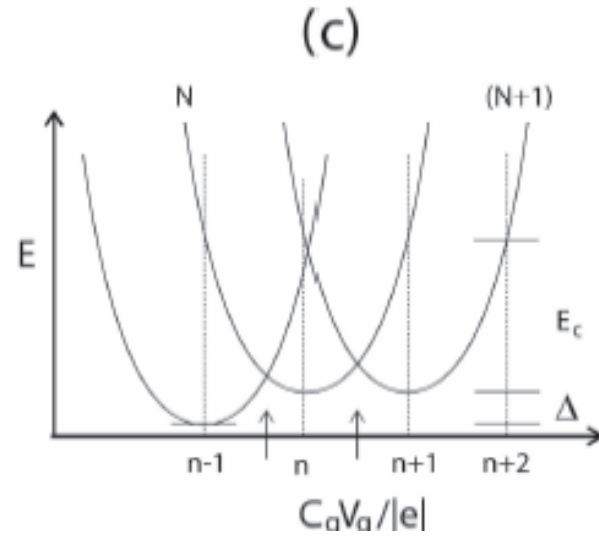
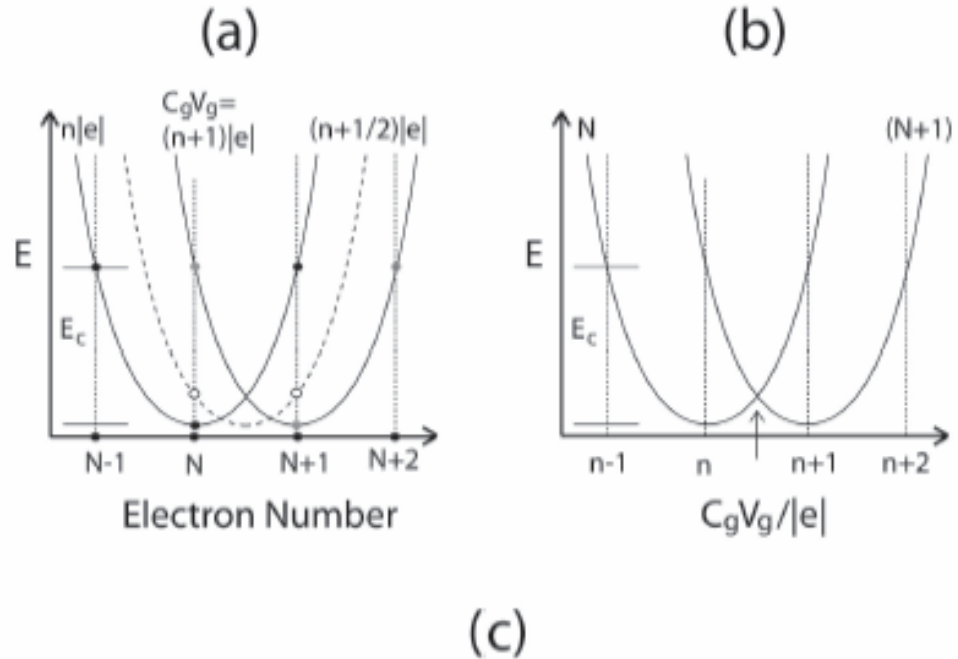
(b)





$$E = \frac{Q^2}{2C} - \frac{C_g}{C} Q V_g,$$

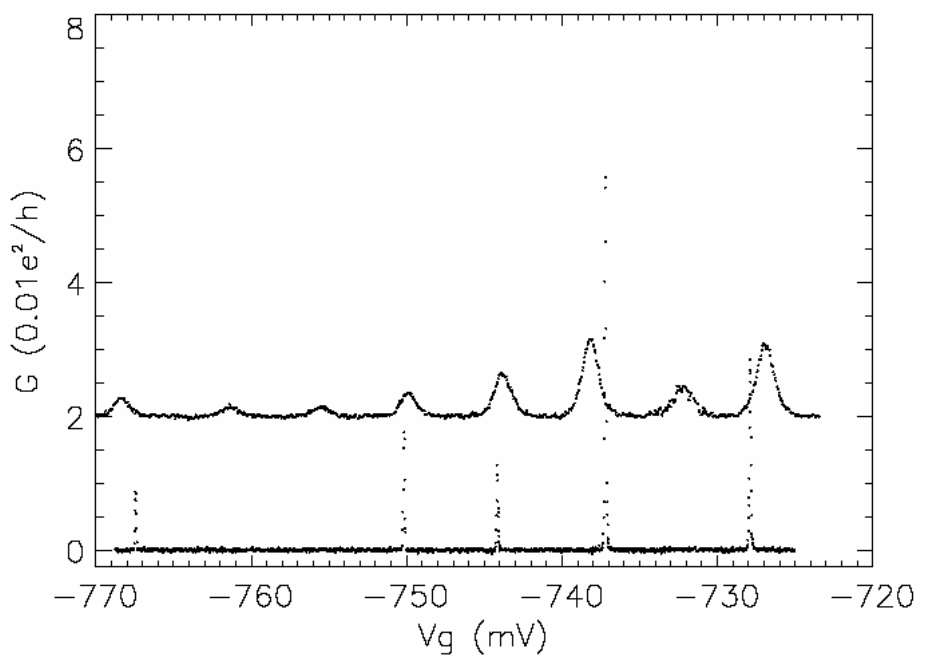
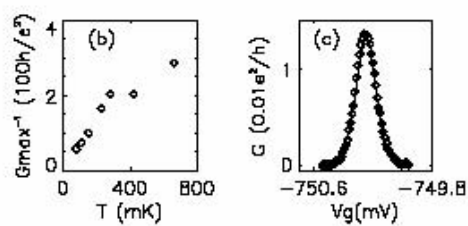
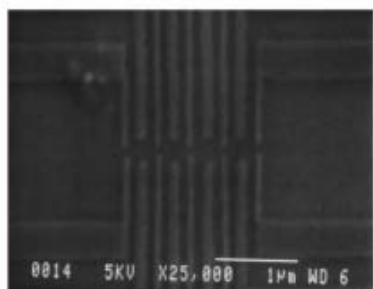
$$E = \frac{(-N|e| + C_g V_g)^2}{2C} - \frac{C_g^2}{2C} V_g^2,$$



$$I(kT, eV_{bias}) = \frac{e^2}{h} \int dE [f(E + eV_{bias}) - f(E)] \frac{\Gamma_L \Gamma_R}{\Gamma^2 + (E - E_o)^2}. \quad (4)$$

$$G_{\max} = \frac{e^2}{h} \frac{\pi}{2kT} \frac{\Gamma_L \Gamma_R}{\Gamma_L + \Gamma_R}$$

$$\Gamma \ll kT \ll \Delta$$

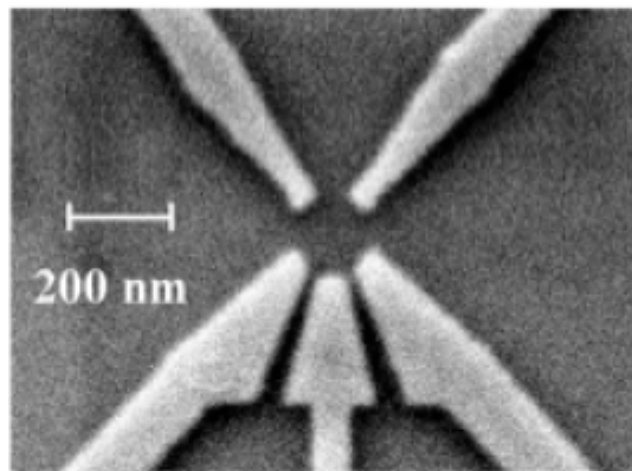
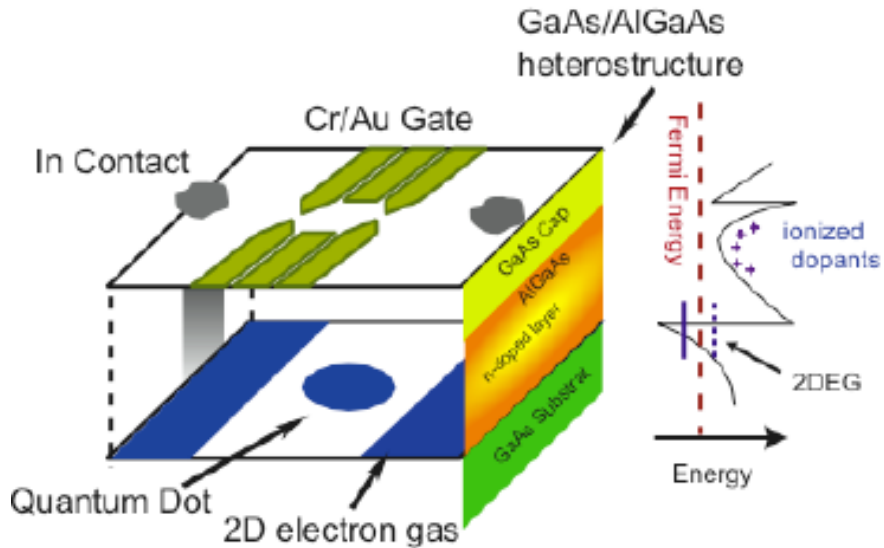


$$-\partial f / \partial \epsilon$$

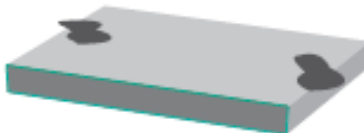
Fabrication Techniques

- Advanced Electron Beam Lithography
- Self-Assembly/chemical growth
- Template
- NanoImprint
- Exfoliation--Graphene

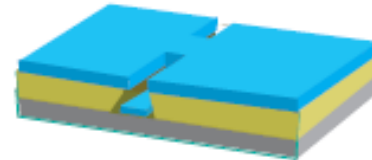
Quantum Dots! (Robust Qubits)



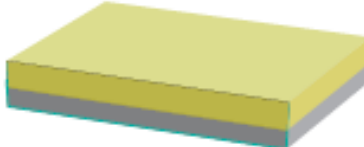
(a) Anneal Contact



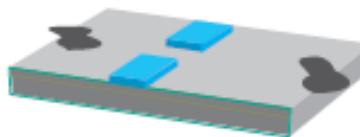
(e) Evaporate Au/Cr



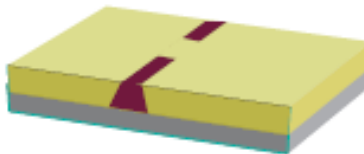
(b) Spin PMMA



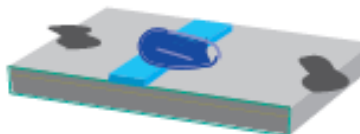
(f) Lift-off



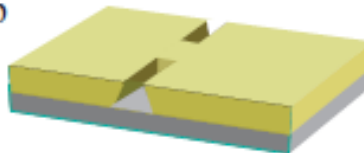
(c) e-Beam



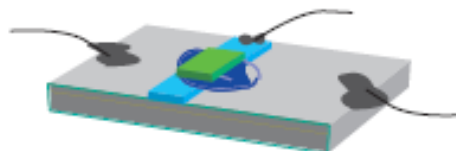
(g) Over-exposure PMMA



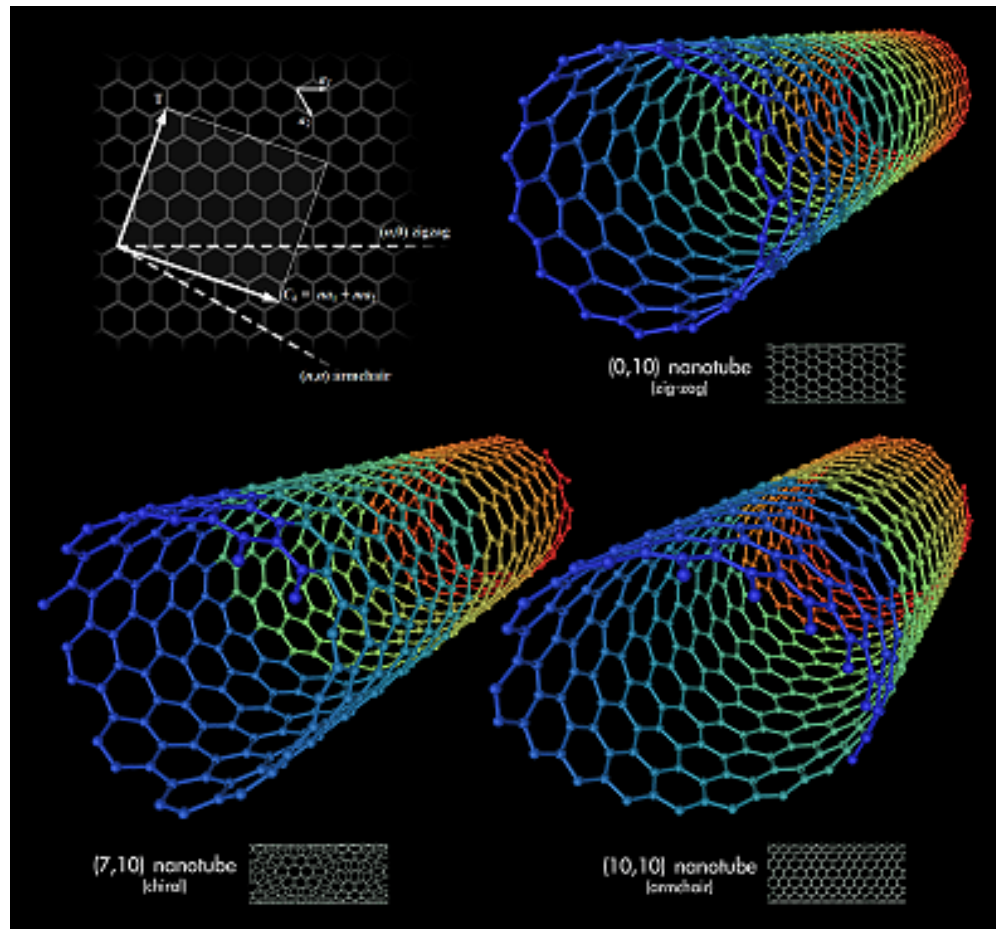
(d) Develop



(h) Bridge and Wire

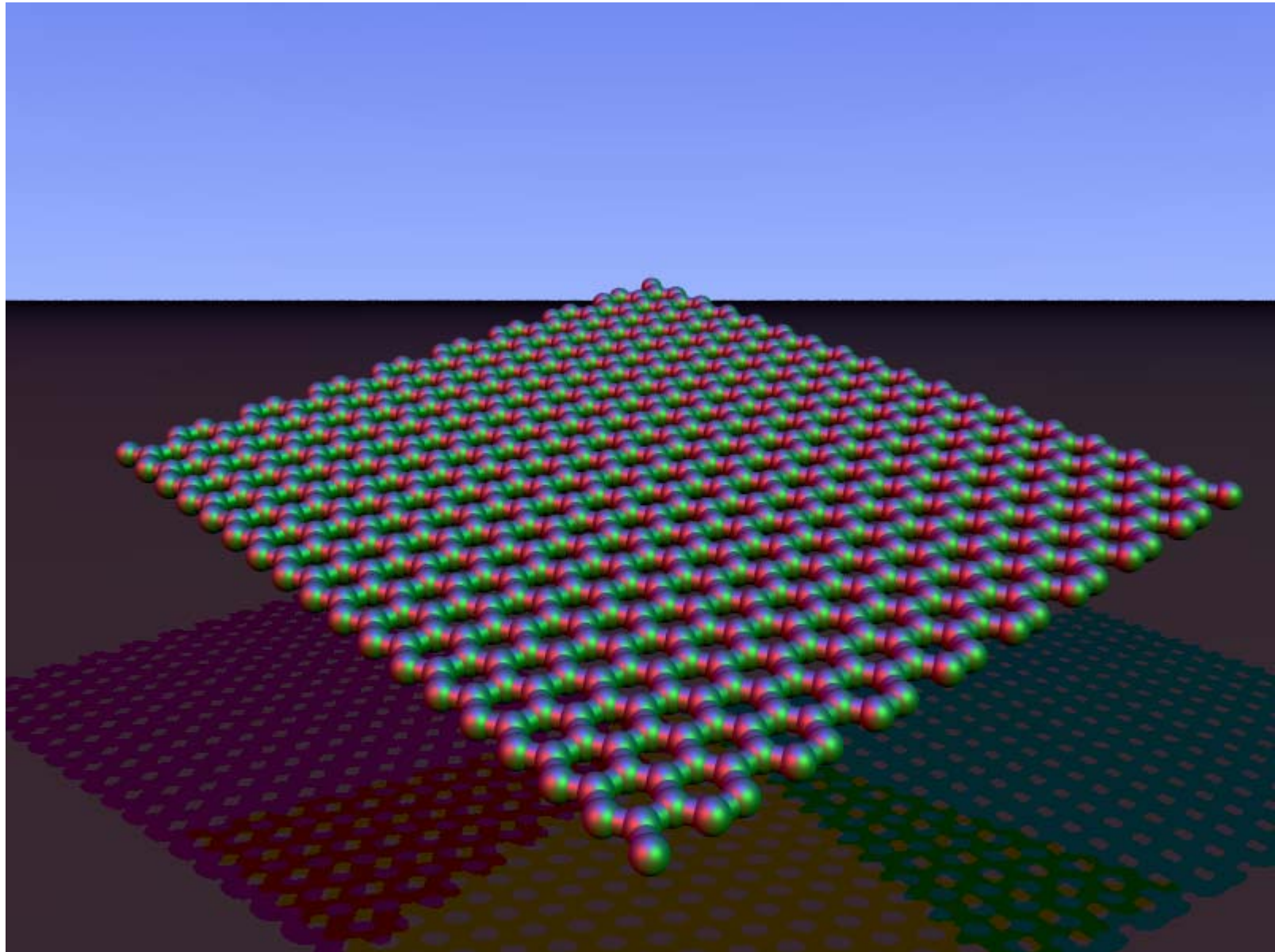


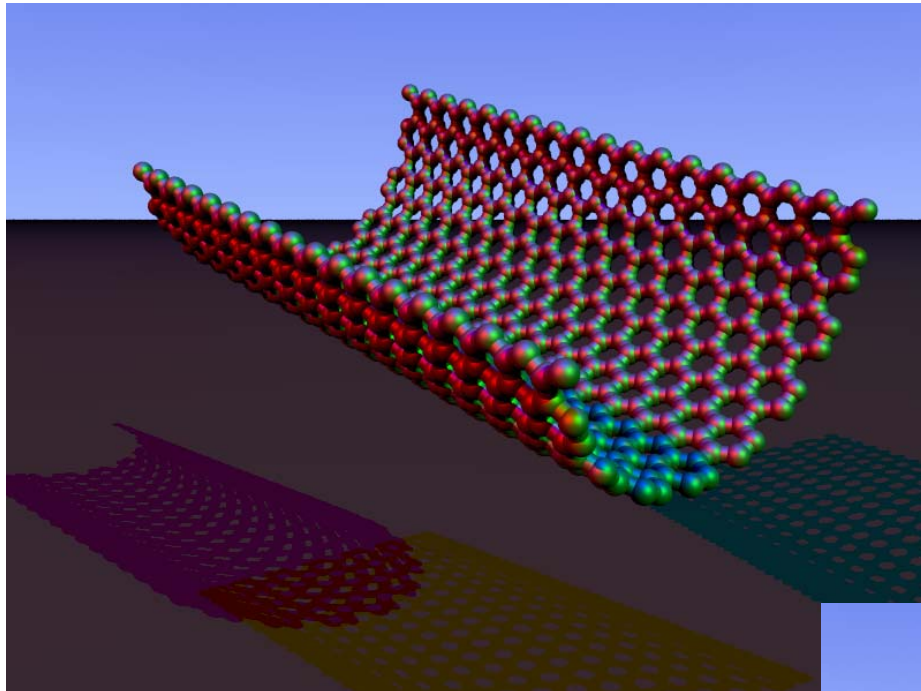
Self-Assembly



Graphene Sheet

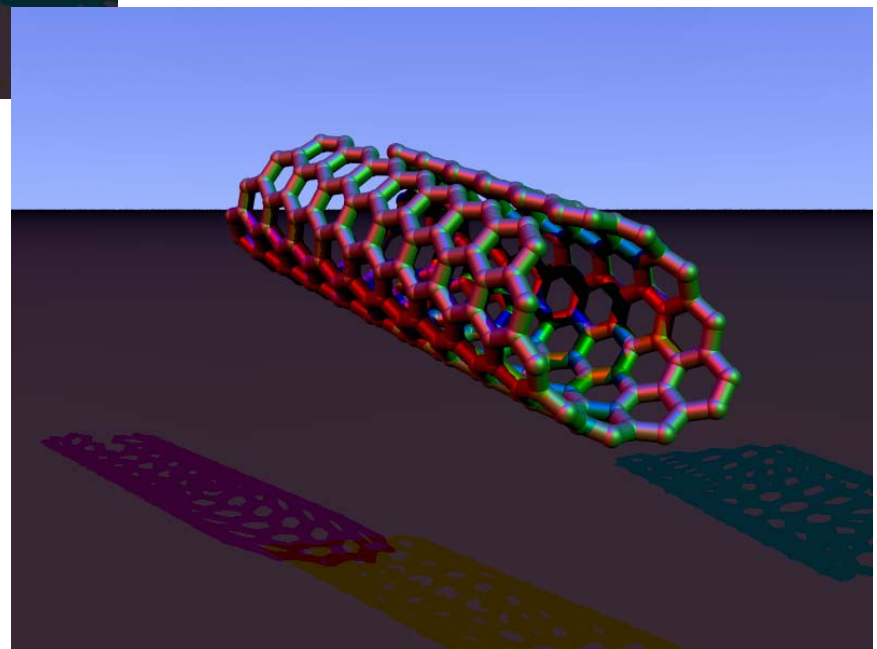
AK Geim; P. Kim





Armchair--Metallic

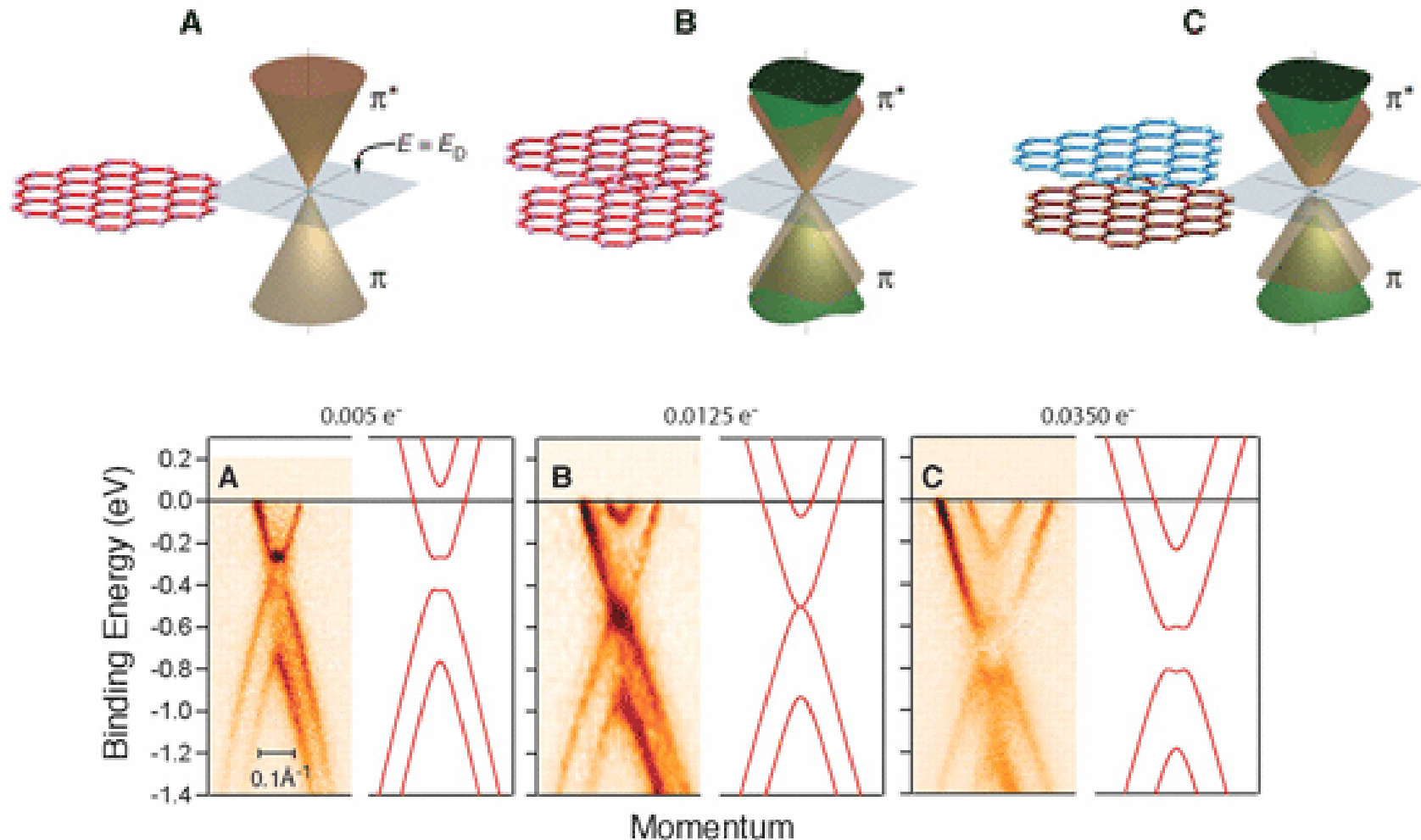
Zigzag--
Semiconducting



Comparison of Mechanical Properties^{[26][27][28][29][30][31][32]}

Material	<u>Young's Modulus</u> (TPa)	Tensile Strength (GPa)	Elongation at Break (%)
SWNT	~1 (from 1 to 5)	13-53 ^E	16
Armchair SWNT	0.94 ^T	126.2 ^T	23.1
Zigzag SWNT	0.94 ^T	94.5 ^T	15.6-17.5
Chiral SWNT	0.92		
MWNT	0.8-0.9 ^E	150	
<u>Stainless Steel</u>	~0.2	~0.65-1	15-50
<u>Kevlar</u>	~0.15	~3.5	~2
Kevlar ^T	0.25	29.6	

Single and Bi-layer Graphene



Self-Assembled Quantum Dots

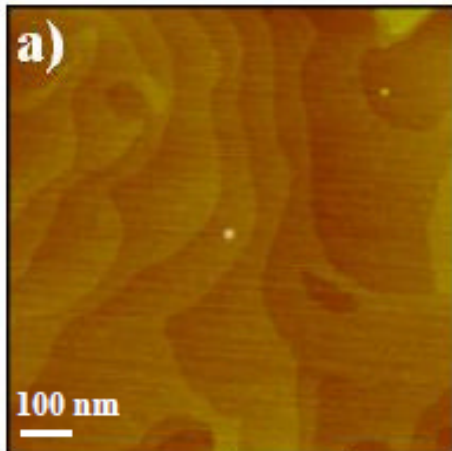
E.g. Gold nanoparticles,
ZnS claded CdSe NP

Size-Sorted Colloidal Nanocrystals

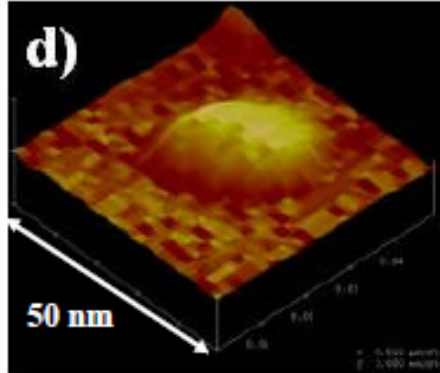
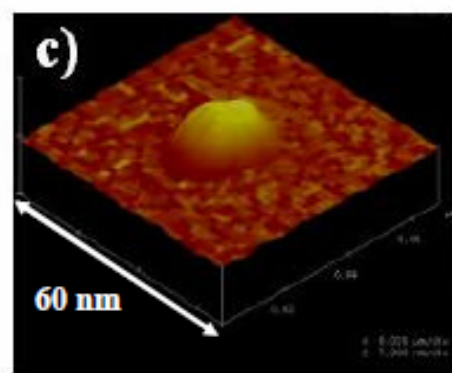
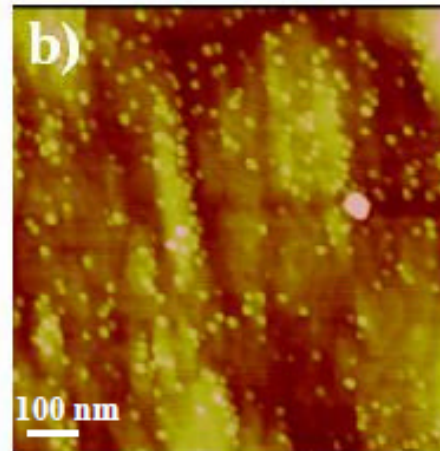


AFM of (110) InAs QDs

(110)



(100)



S. Lyons, Princeton University

Template Superconducting Al Nanowire

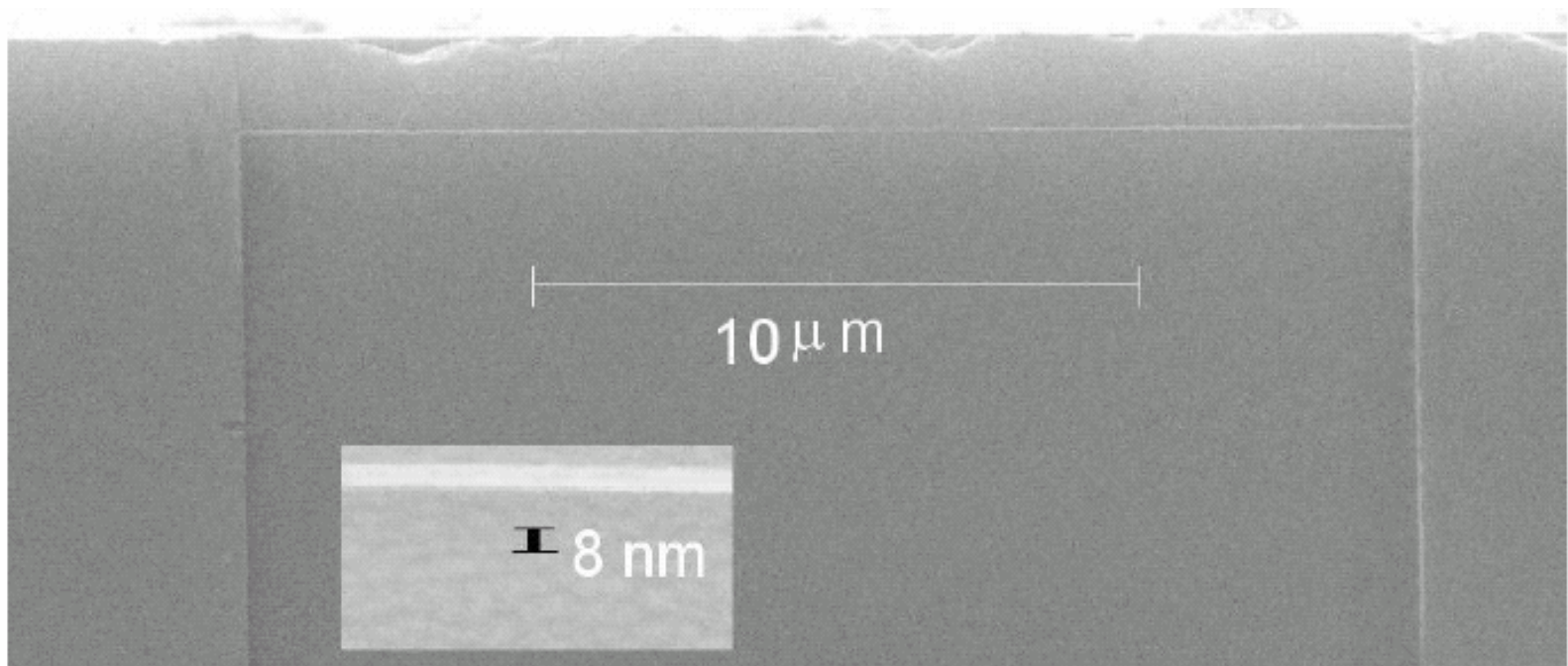
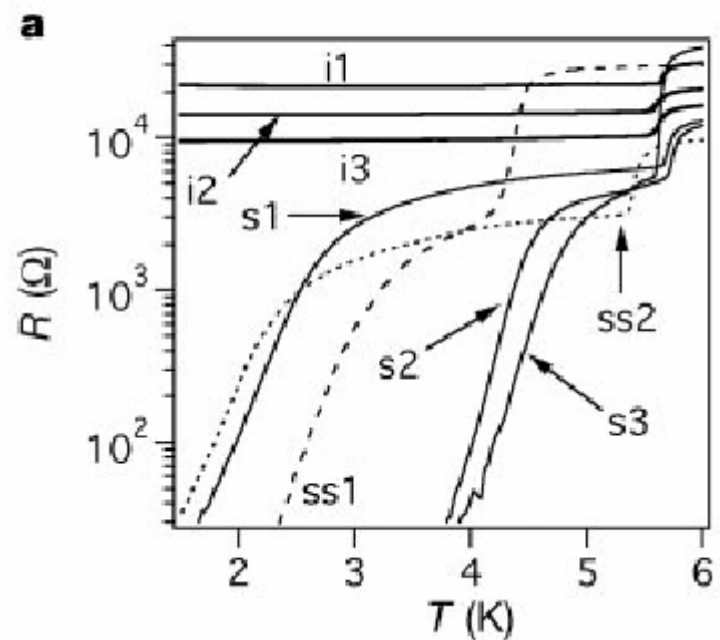
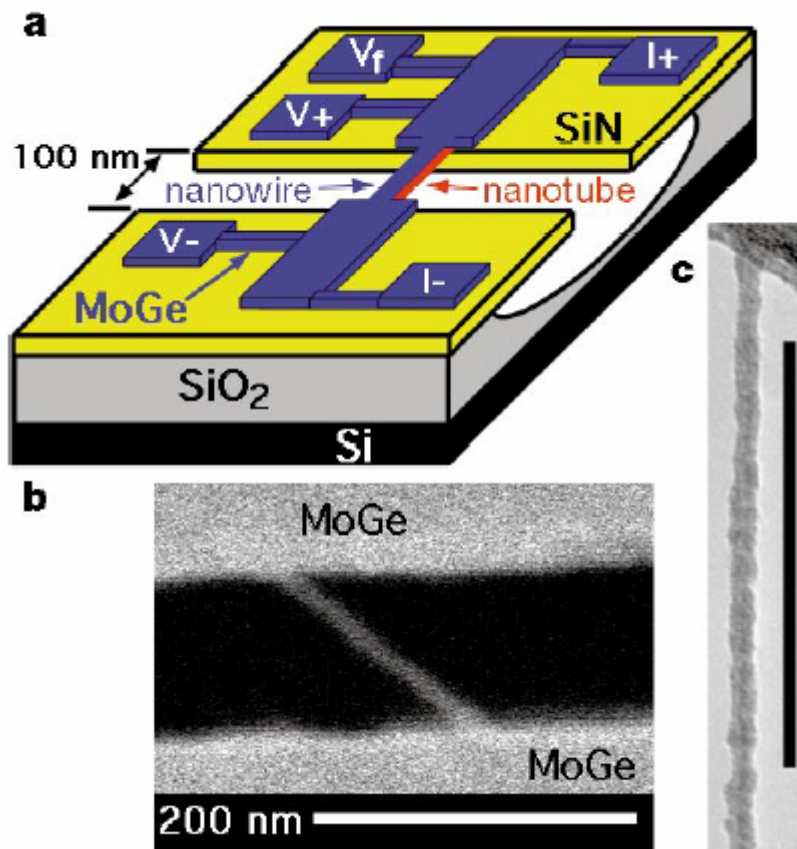


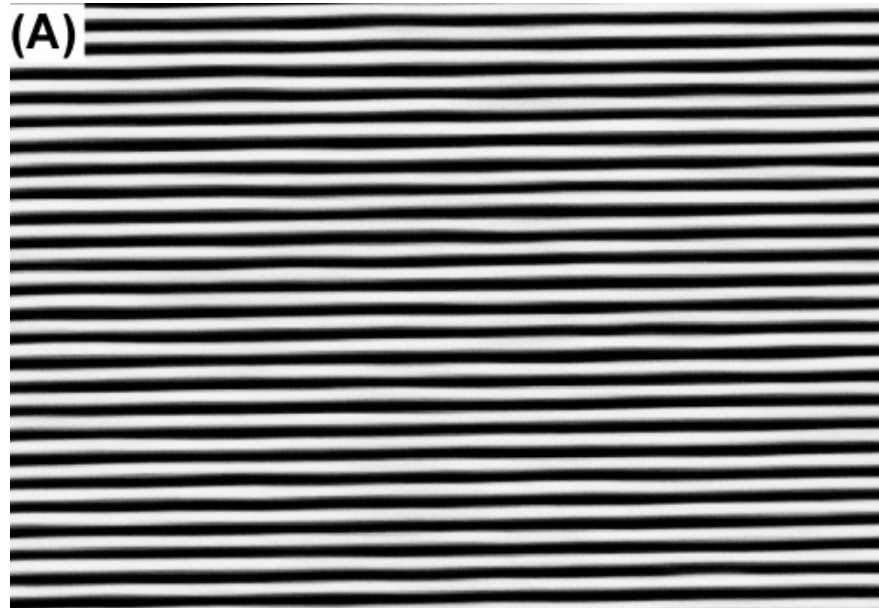
FIG. 2: SEM image of an 8 nm wide wire 20 μm long.

F. Altomare, A.M. Chang et al., APL (2005)

A. Bezryadin, C.N Lau, and M Tinkham,
Nature 404, 971 (2000).

Mo_{0.79}Ge_{0.21}

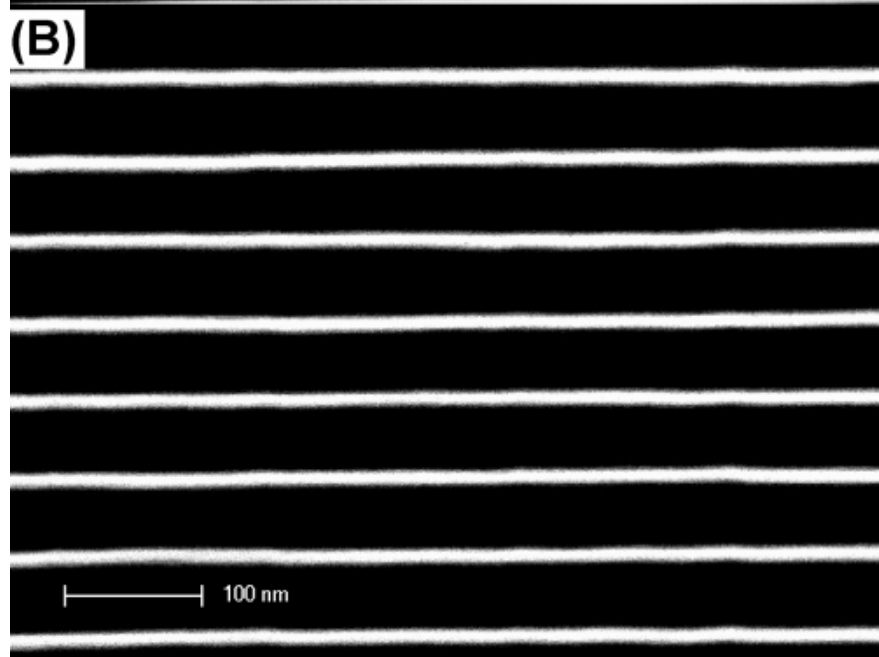




Caltech

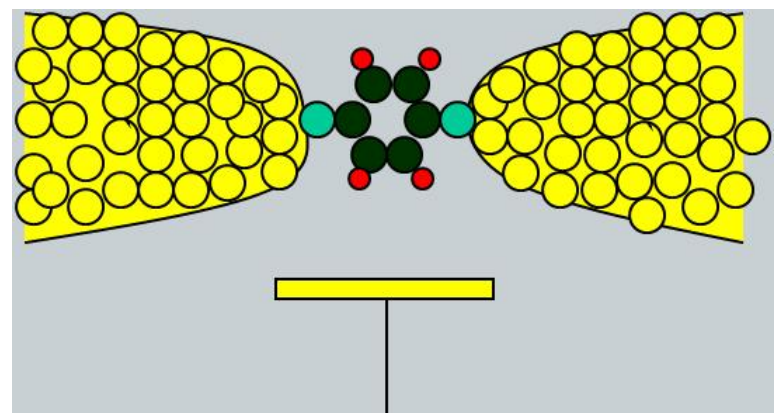
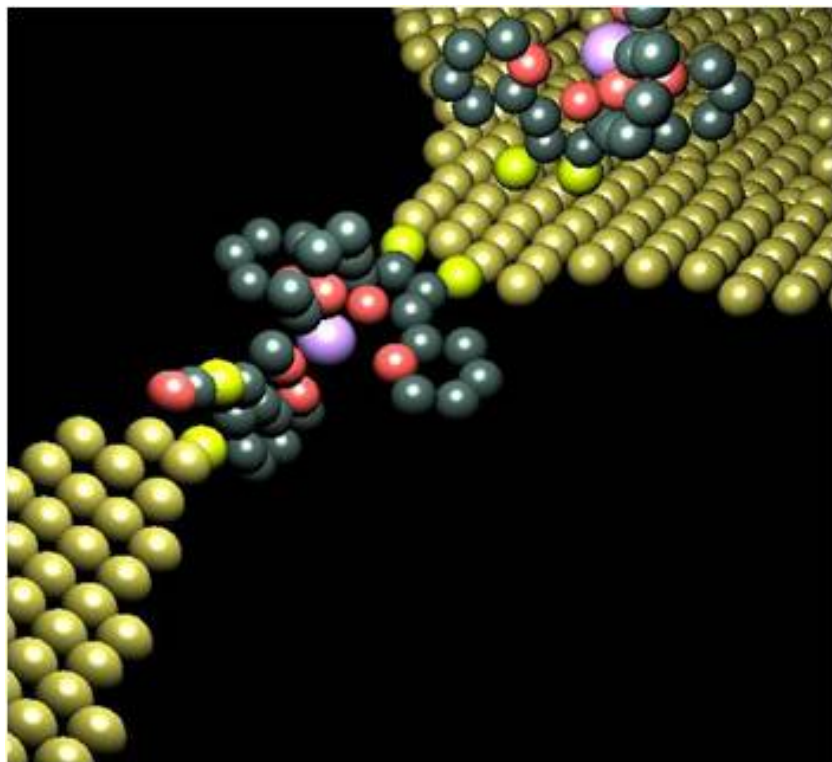
200 nm

EHT = 20.00 kV WD = 3 mm



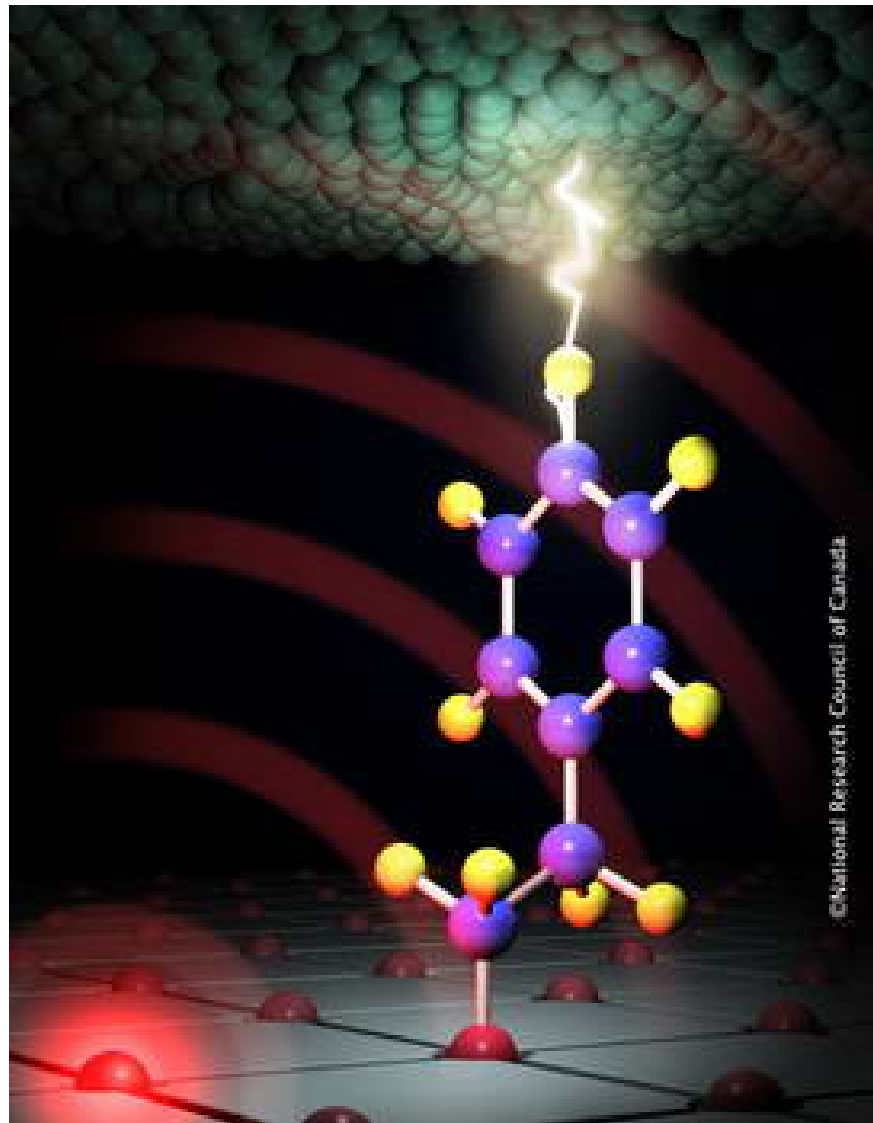
J. Heath, 2008

Combination—e.g. Molecular Devices

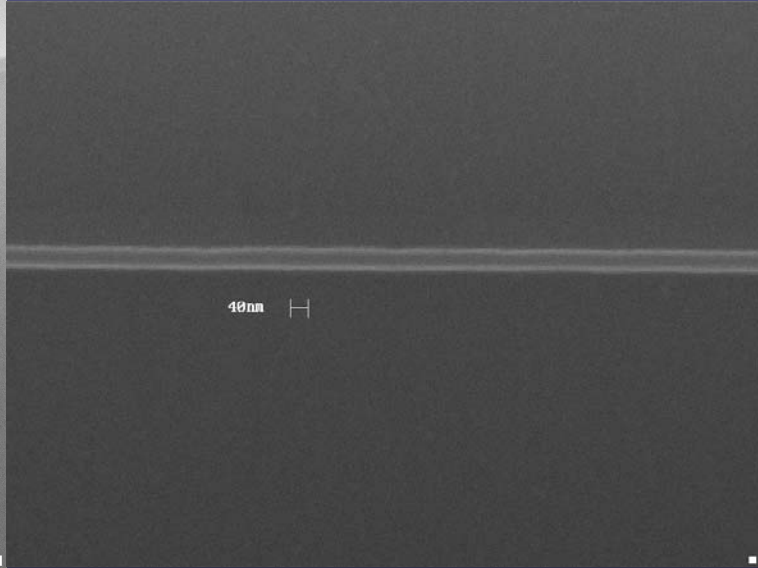
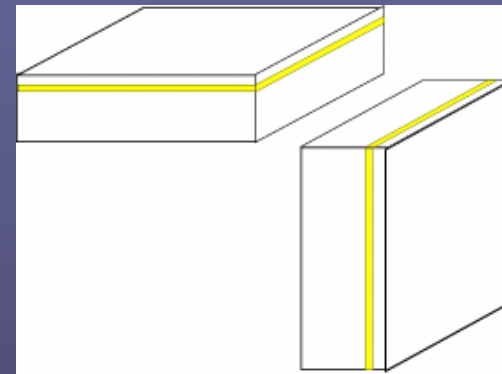
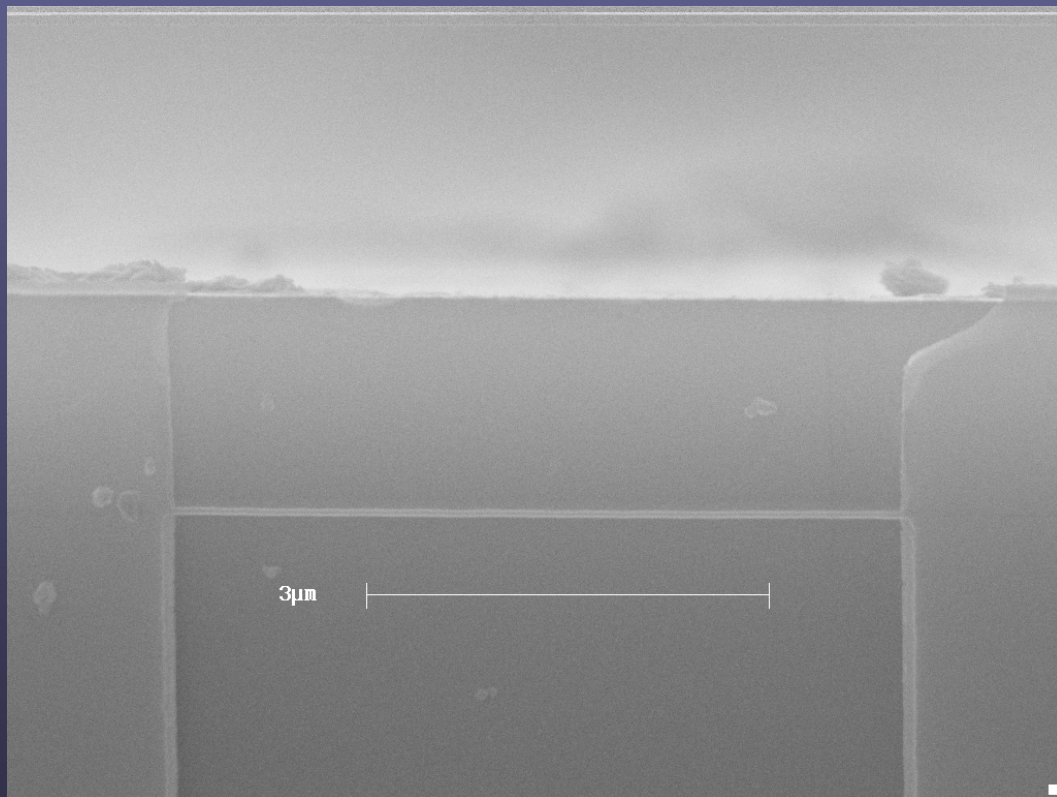


Tetrahydrofuran (THF)
Natelson (Rice);
image: J.W. Ciszek

©National Research Council of Canada



Metallic Nanowire



Superconducting Al Nanowire

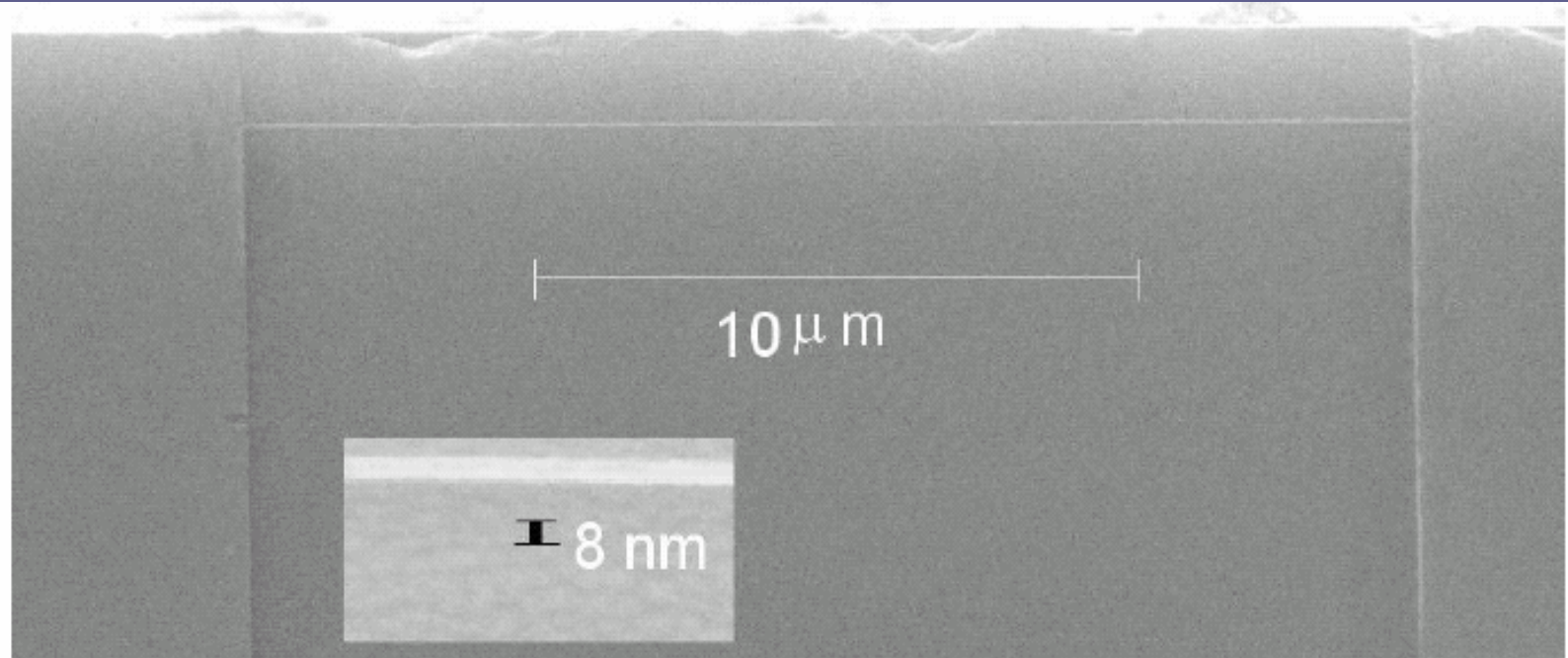
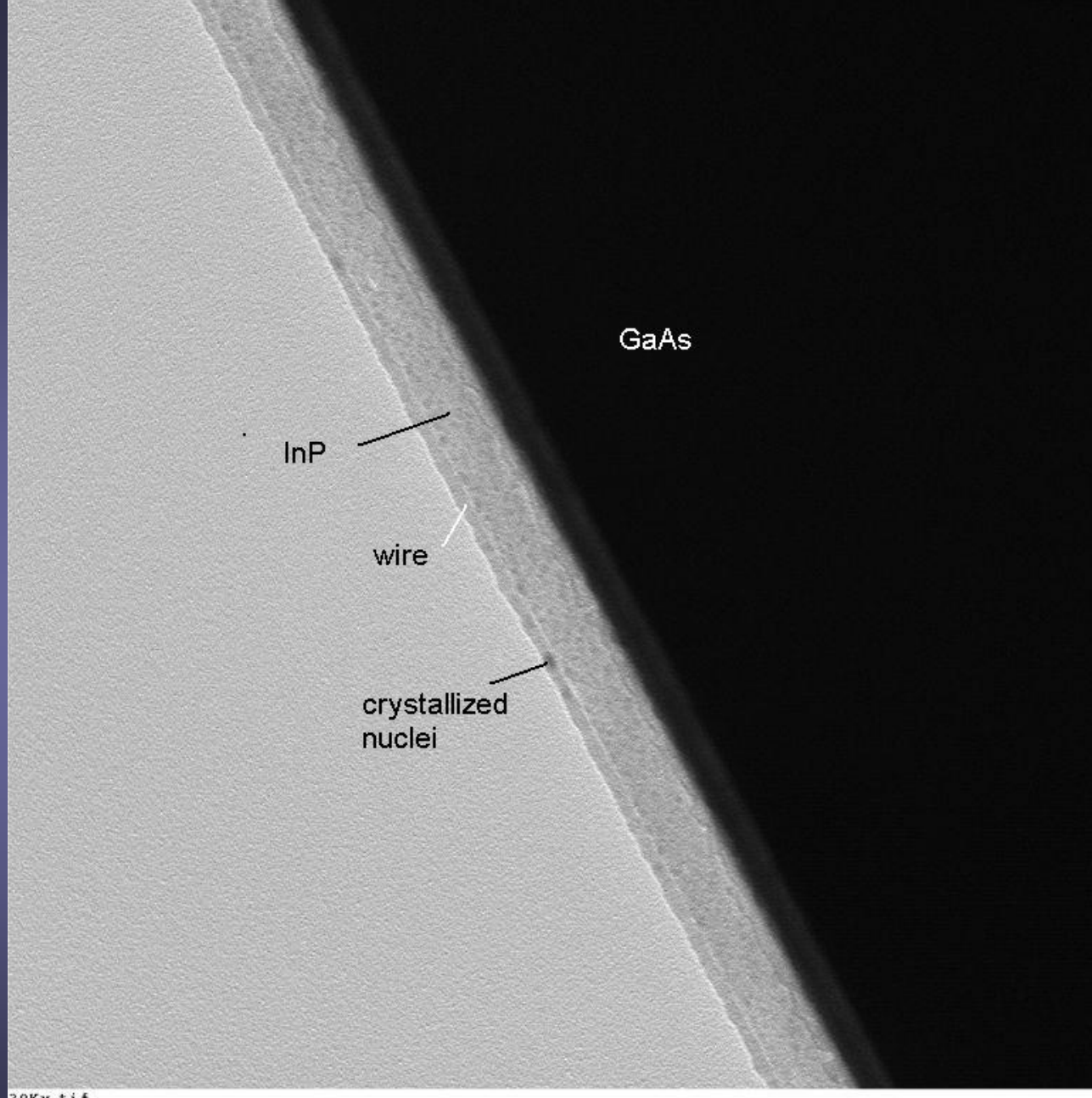
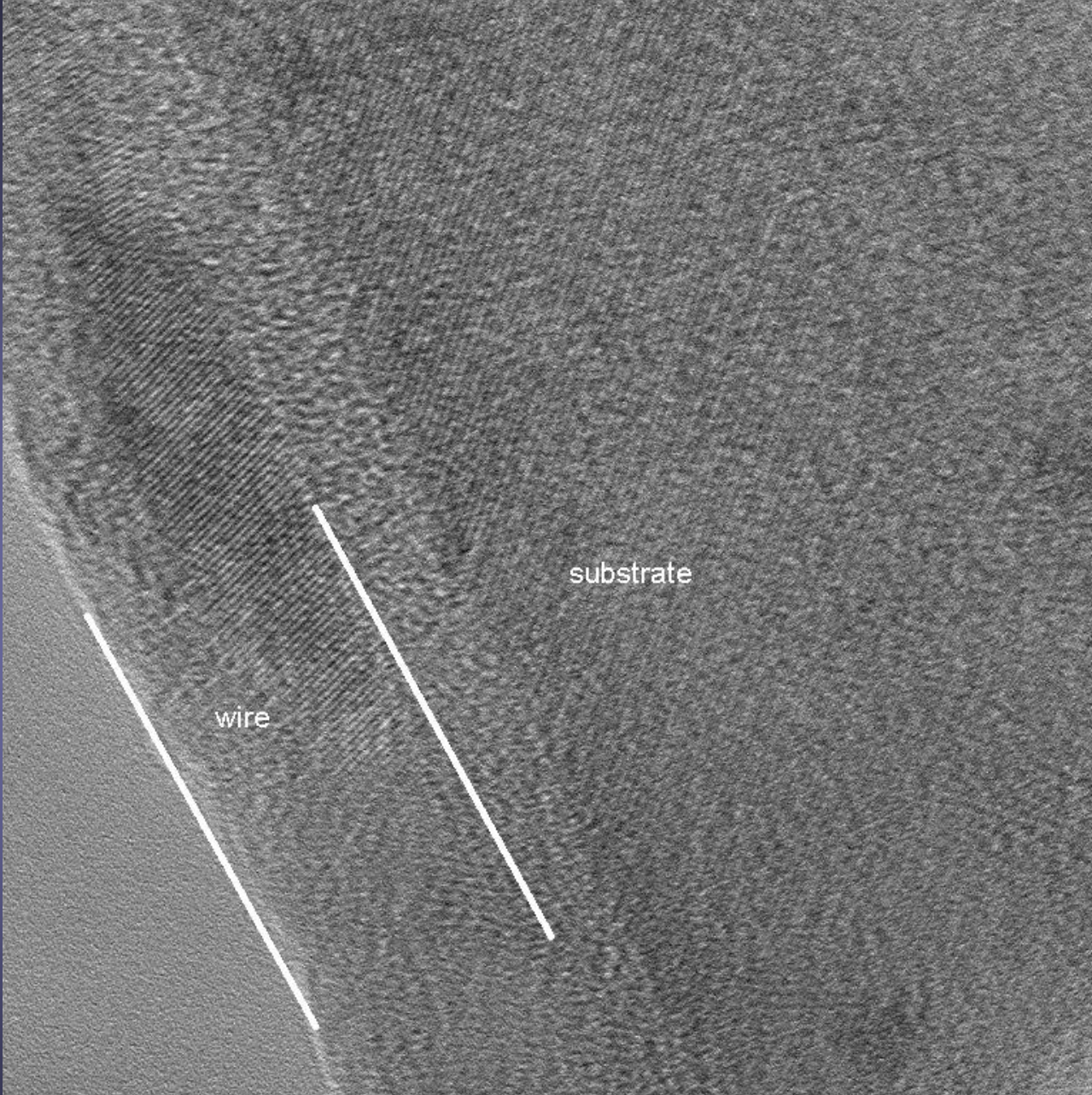


FIG. 2: SEM image of an 8 nm wide wire 20 μm long.



30Kx.tif
Print Mag: 119000x @ 100 mm
14:40 05/18/06

100 nm
HV=200kV
Direct Mag: 30000x
Duke SMiF TEM

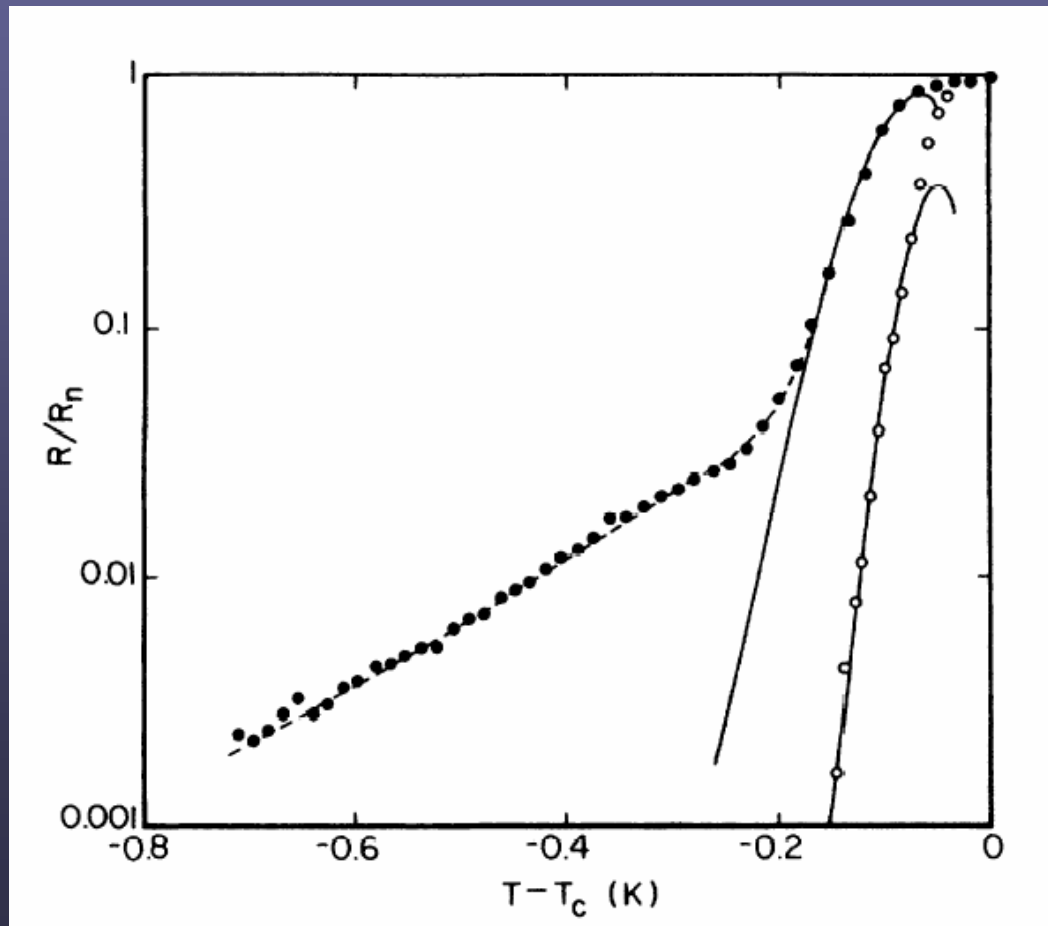


700Kx_1.tif
Print Mag: 2960000x @ 100 mm
15:23 05/18/06

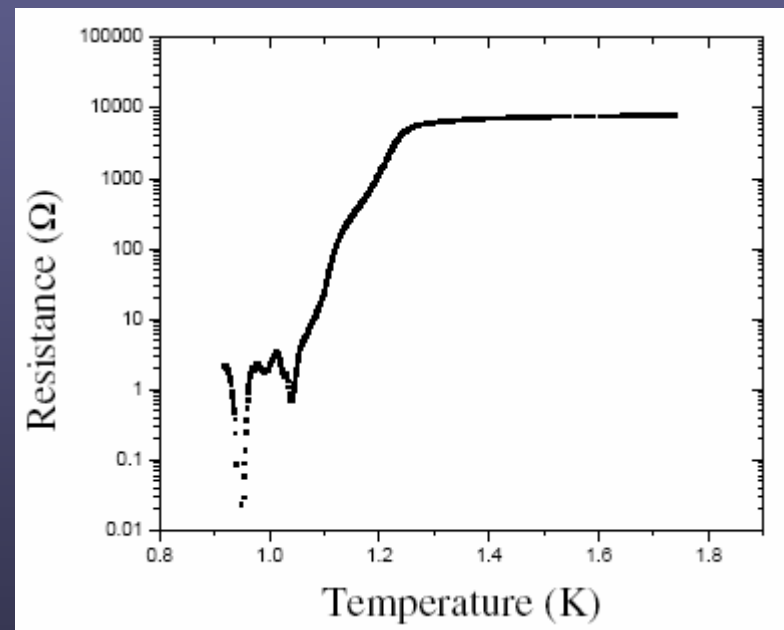
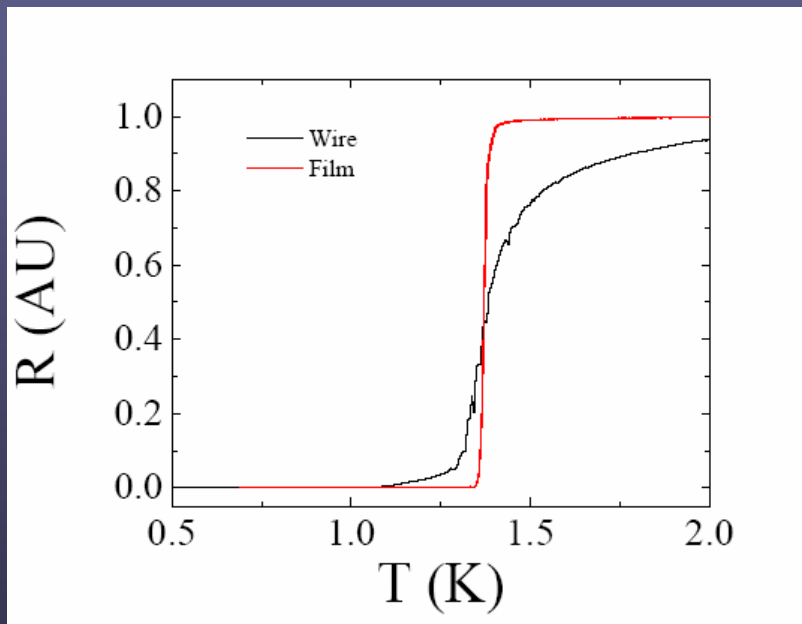
5 nm
HV=200kV
Direct Mag: 700000x
Duke SMiF TEM

N. Giordano
Phys. Rev. Lett. 61, 2137-2140 OCT 31
1988; and Phys. Rev. B 41, 6350 (1990).

41 nm diameter In wire



1D versus 2D Superconductivity



Superconducting ultra-narrow Al nanowires

Fabio Altomare^{1,2}, Albert M. Chang^{1,2},
Michael R. Melloch³,
Yuguong Yang⁴, Charles W. Tu⁴

1) Dept. of Physics, Purdue University

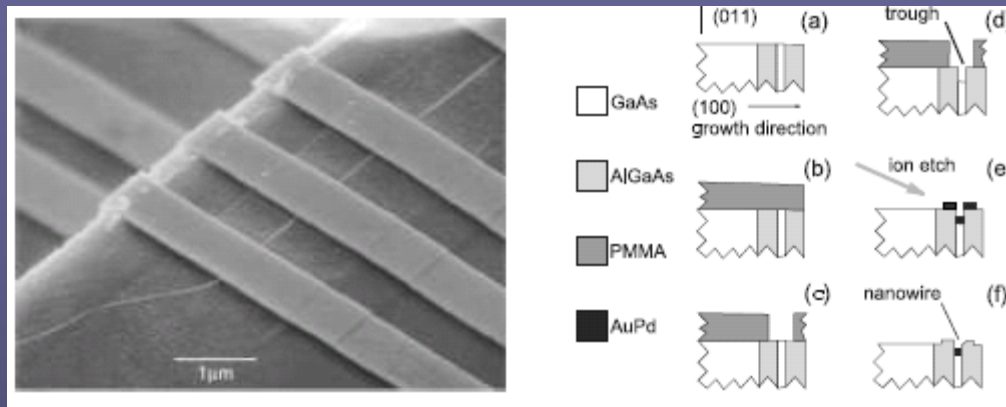
2) Dept. of Physics, Duke University

3) School of Electrical and Computer Engineering, Purdue University

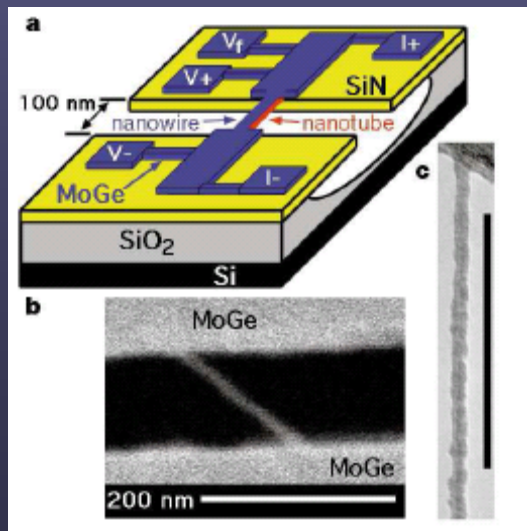
4) Dept. of Computer and Electrical Engineering, UCSD

Partially supported by NSF DMR-0135931 DMR-0401648

State of the art techniques

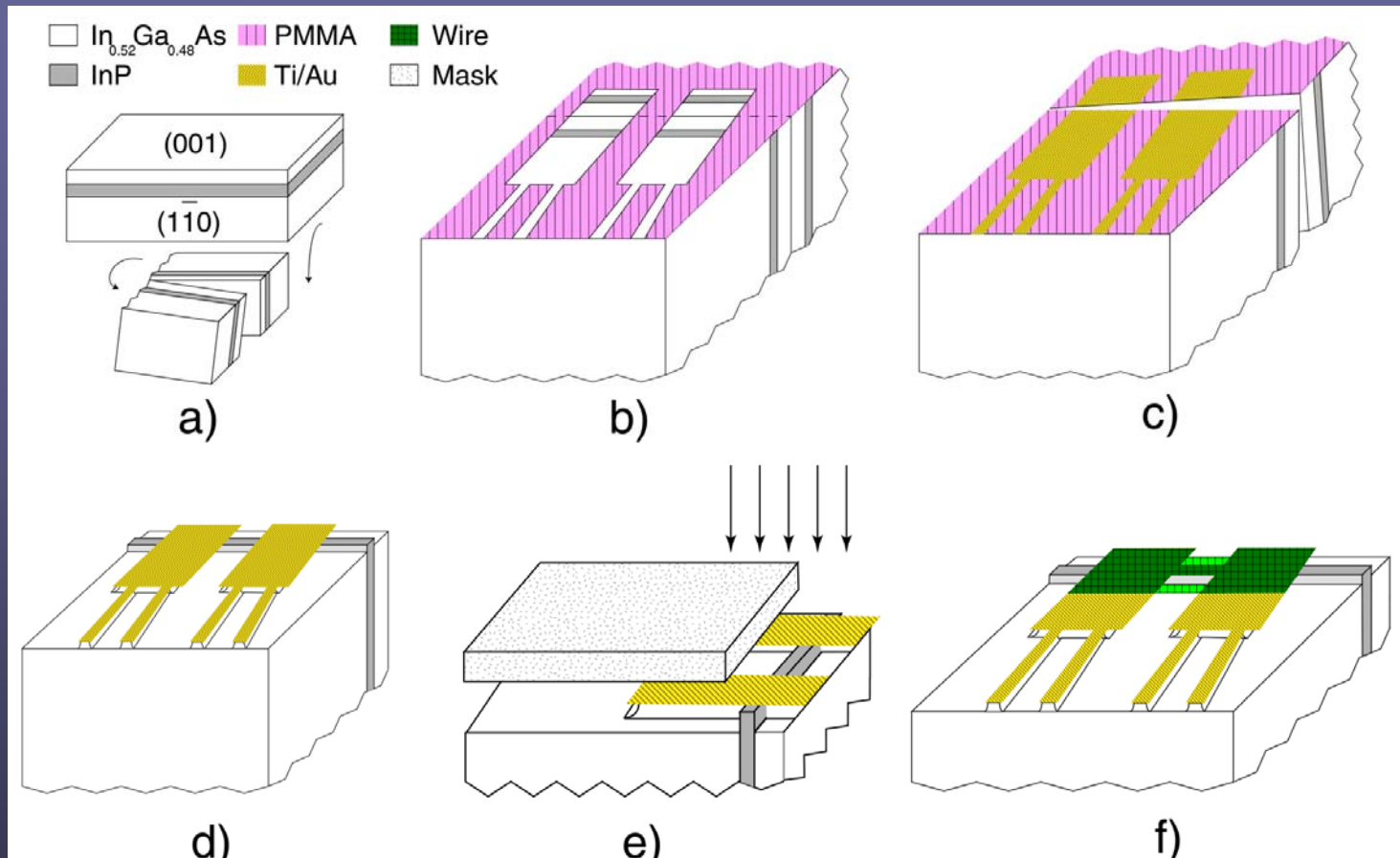


Natelson *et al.*,
Appl. Phys. Lett. **77**,
1991-1993 (2000)



Bezryadin *et al.*,
Nature **404**,
971-973 (2000)

Fabrication scheme

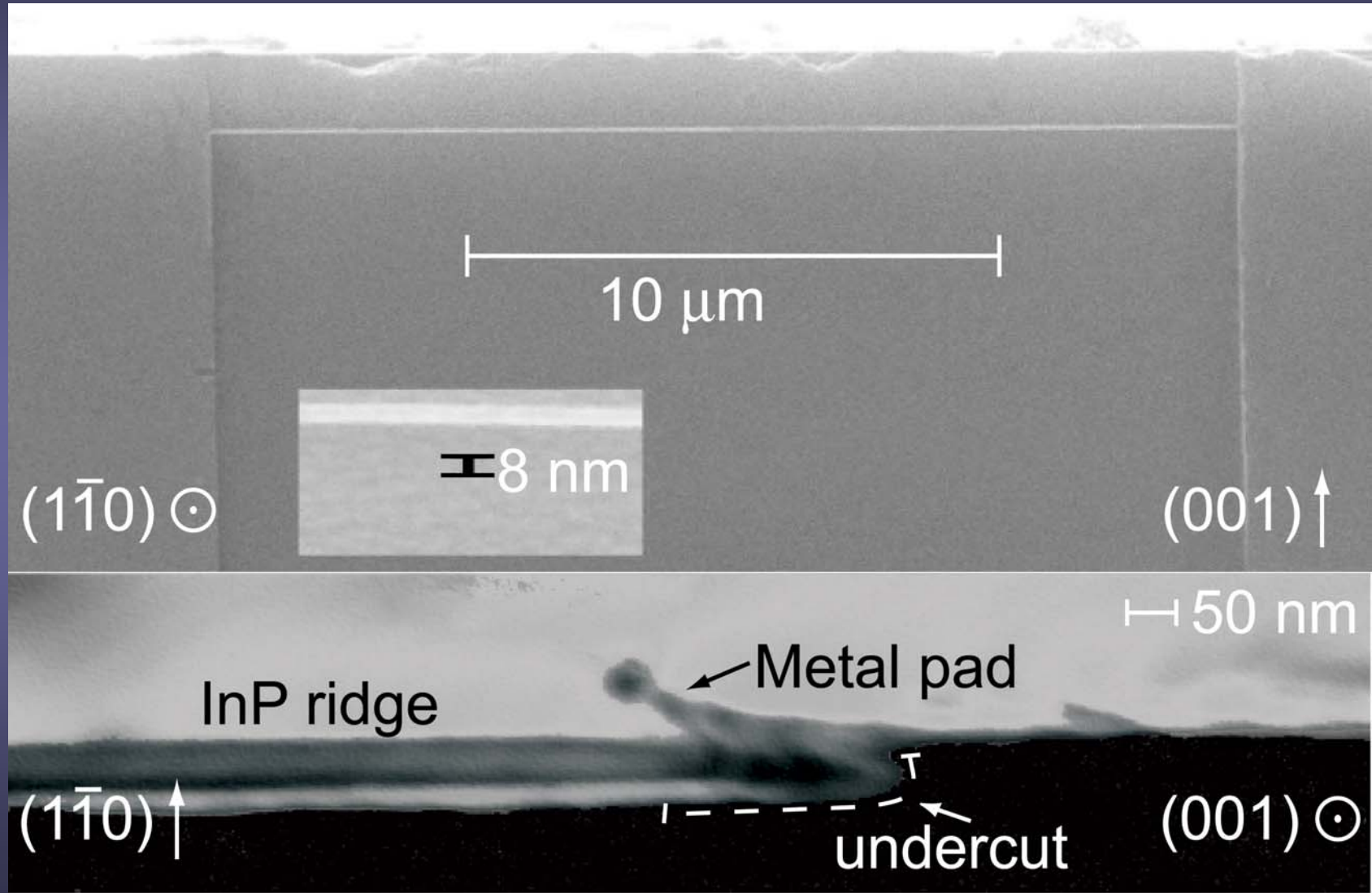


a) Sample preparation
d) Wet etching

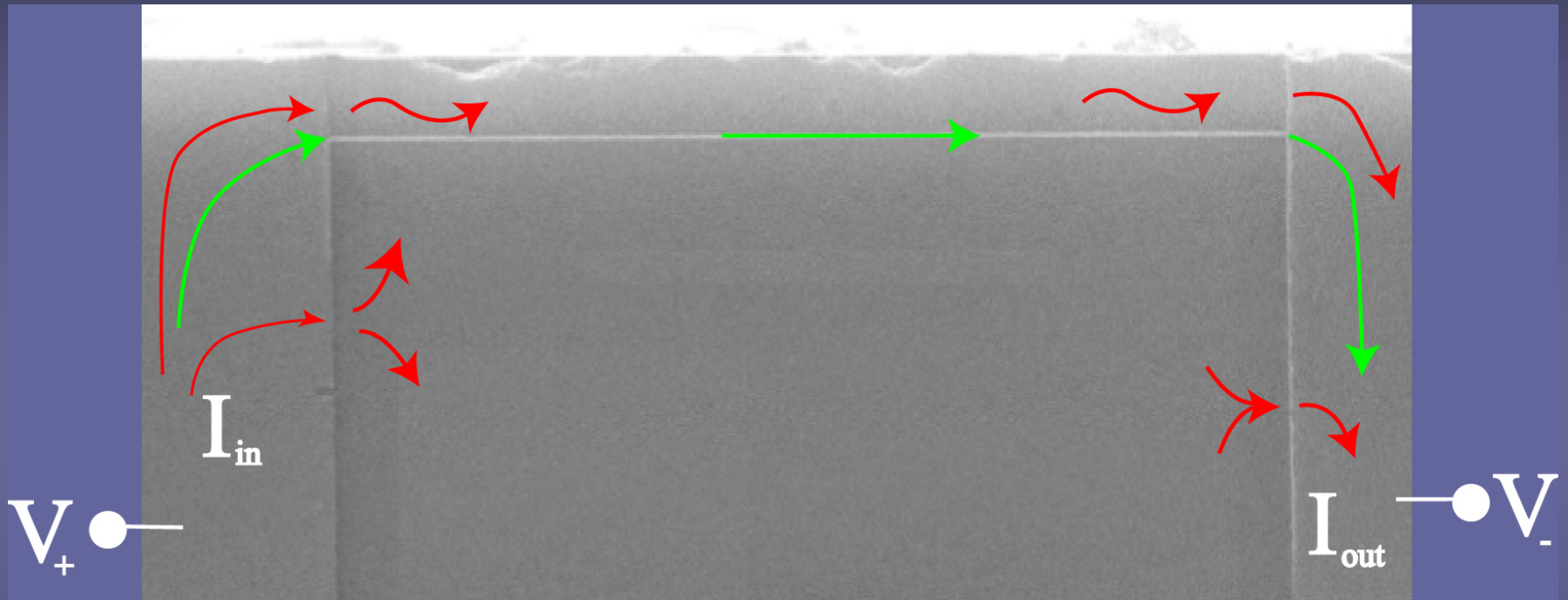
b) Lithography
e) Final evaporation

c) Evaporation
f) Final result

SEM image

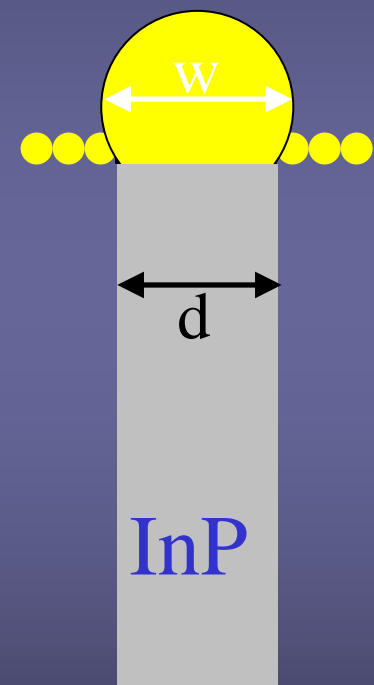
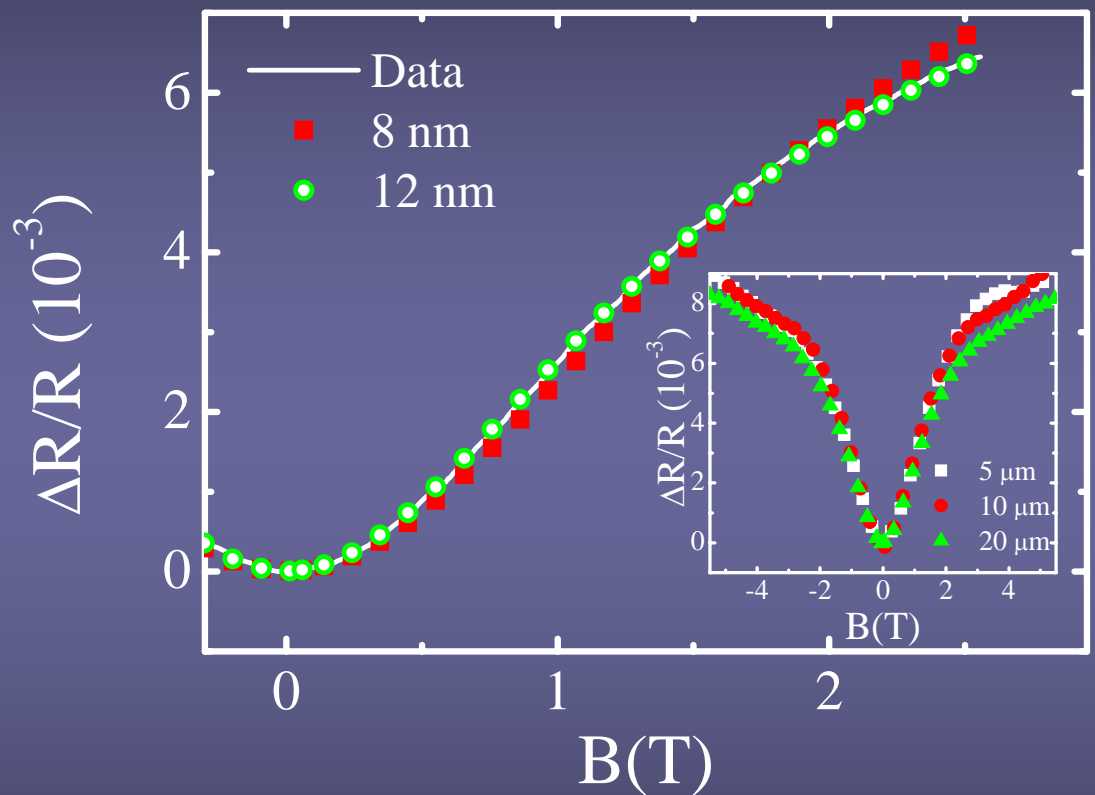


Weak Localization Magnetoresistance



$$\frac{\Delta R}{R} = \frac{e^2}{\pi h} \frac{R}{L} \left[\frac{3}{2} \left(\frac{1}{L_\phi^2} + \frac{4}{3L_{so}^2} + \frac{w^2 e^2}{3h^2} B^2 \right)^{-1/2} - \frac{1}{2} \left(\frac{1}{L_\phi^2} + \frac{w^2 e^2}{3h^2} B^2 \right)^{-1/2} \right]$$

AuPd wires

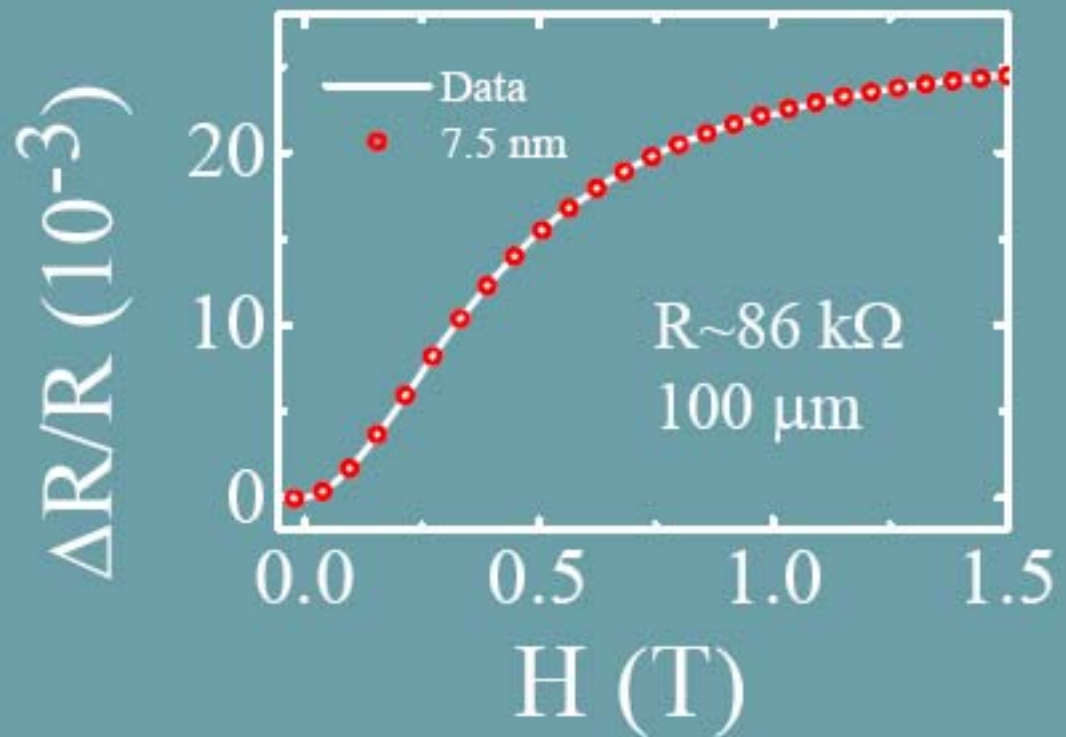


$L=5, 10, 20 \mu\text{m}$
 $R=20, 35, 70 \text{ k}\Omega$

$w = 8 \text{ nm}$
 $L_\phi = 99 \text{ nm}$

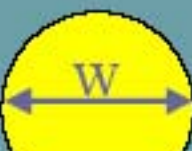
$w = 12 \text{ nm}$
 $L_\phi = 81 \text{ nm}$

Al nanowires



$$w = .5 \text{ nm}$$

AuPd



$$d$$

InP

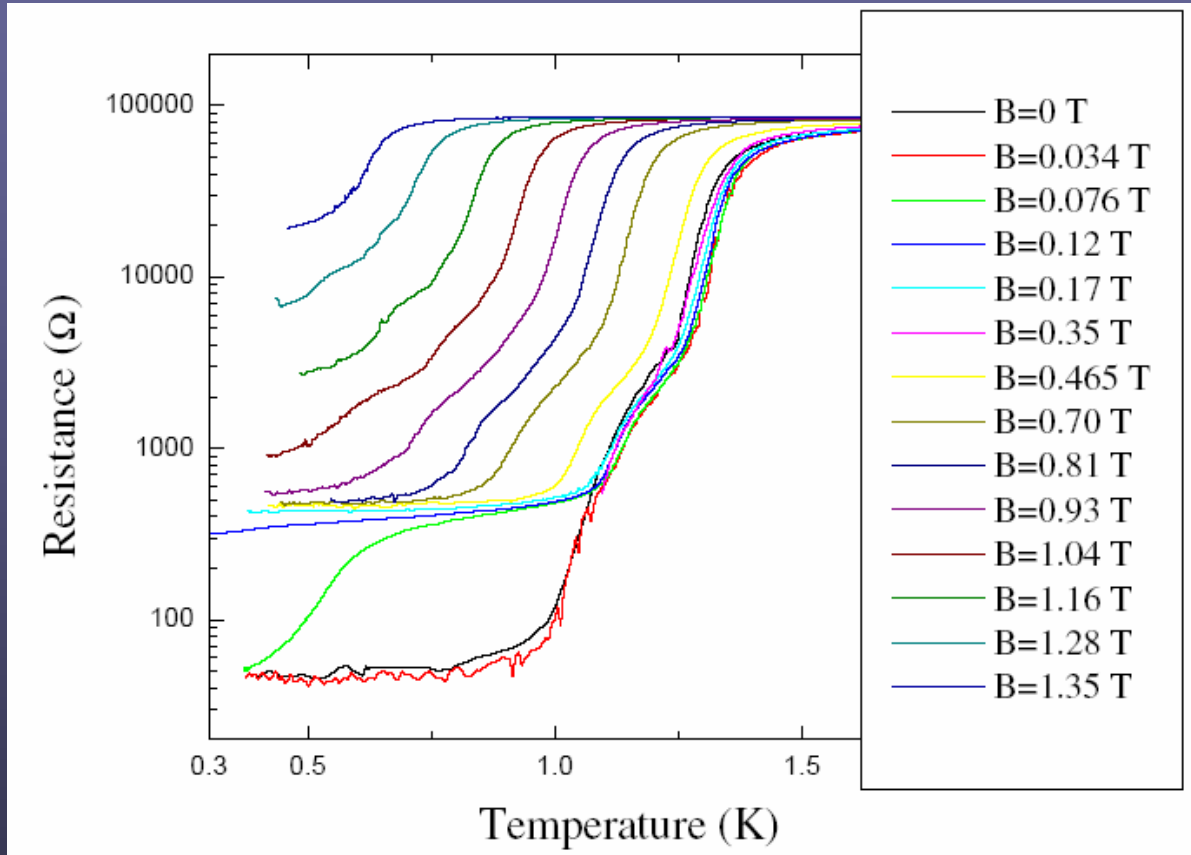
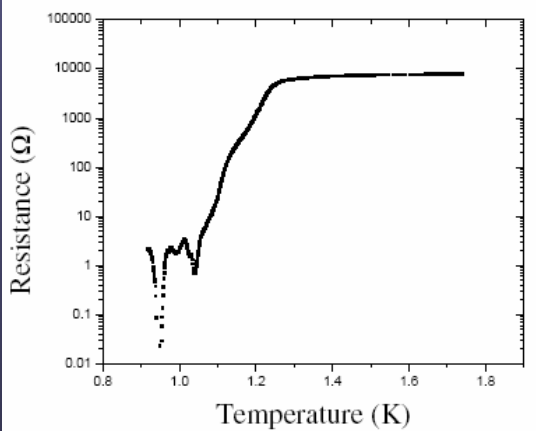
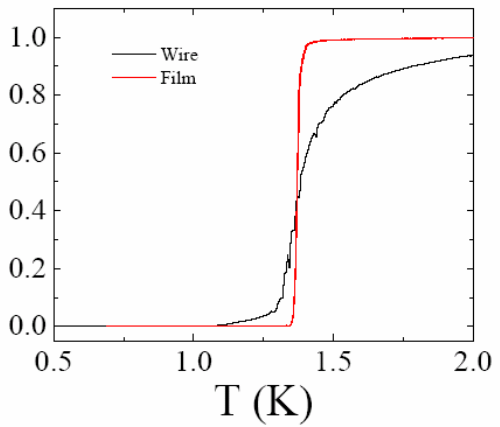
Al



$$d$$

InP

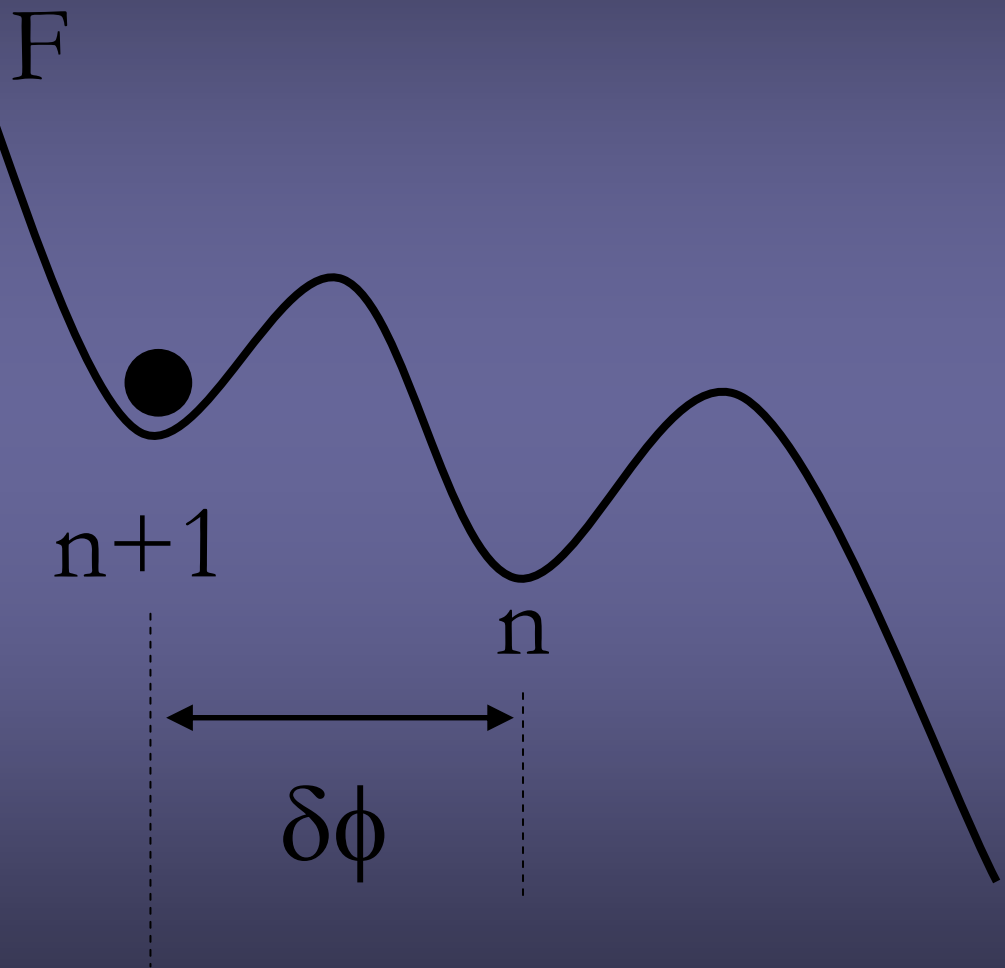
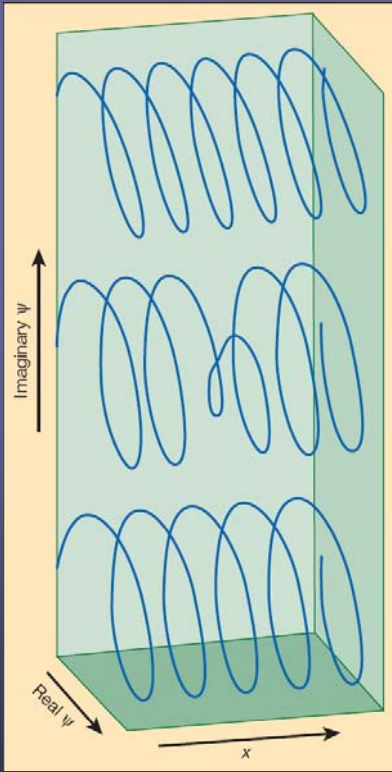
R (AU)

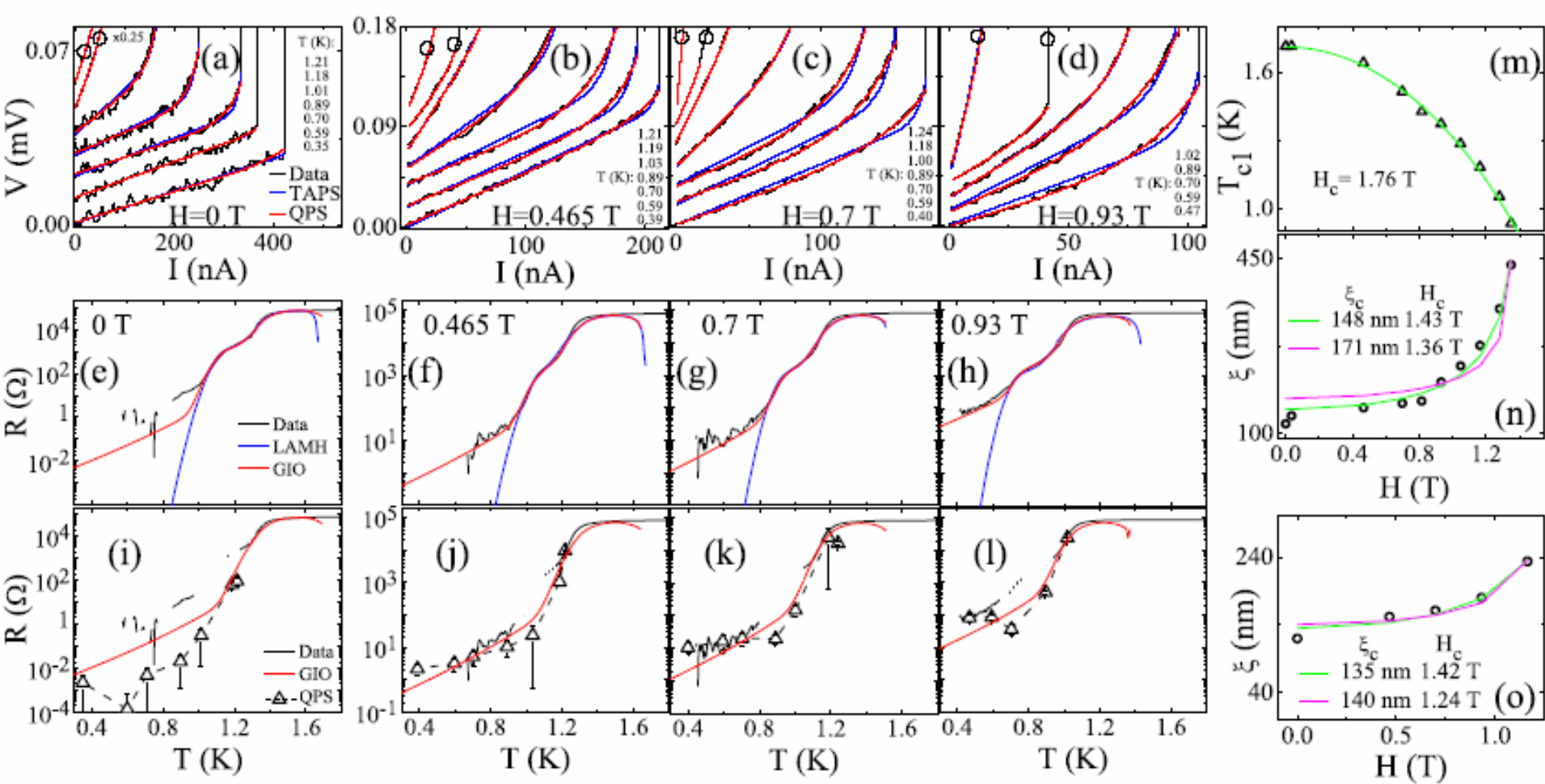


Model of a superconducting wire

$$\psi = fe^{ikx}$$

$$k = 2n\pi/L$$





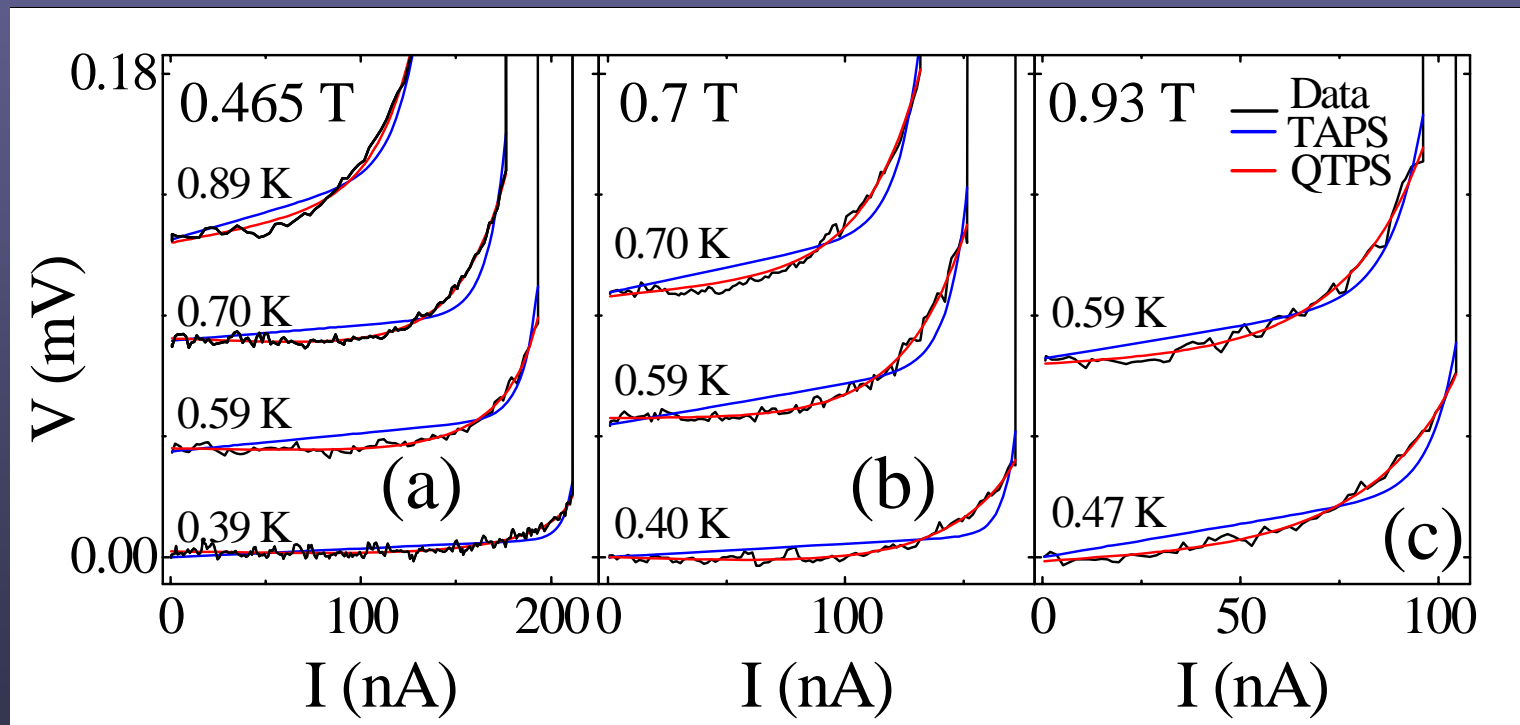
$$R_{LAMH} = R_q \frac{\Omega}{kT} \exp\left(-\frac{\Delta F}{k_B T}\right) \quad R_{GZ} = B_{GIO} R_q \frac{l}{\xi} \sqrt{\frac{\Delta F}{h/\tau_{GL}}} \exp\left(-a_{GIO} \frac{\Delta F}{h/\tau_{GL}}\right)$$

$$\Omega = \frac{L}{\xi} \left(\frac{\Delta F}{kT} \right)^{\frac{1}{2}} \frac{1}{\tau_{GL}}, \quad \Delta F = \frac{8\sqrt{2}}{3} \frac{H_c^2}{8\pi} A \xi$$

Non-linear V-I

$$V_{LAMH} = R_{TAPS} I_0 \sinh(I/I_0)$$

$$V_{GIO} = R_{QTPS} I_{GIO} \sinh(I/I_{GIO})$$



Power Law dependence

$$\lim_{I \rightarrow \infty} V \propto I^\nu$$

$$V \propto \frac{1}{(\phi_0 \eta)^{2\nu}} \sinh(I\phi_0\eta)$$

$$\eta \propto \frac{1}{T\pi} \operatorname{arctg} \left(\frac{(2\nu+1)\pi T}{\phi_0 I} \right)$$

S. Khlebnikov unpublished; S. Khlebnikov and L. P. Pryadko, Phys. Rev. Lett. **95**, 107007 (2005)

